Crystal Orbital Displacement Analysis of Interactions in the Solid State. Application to the Study of Host···Guest Interactions in the Hofmann Clathrates

Eliseo Ruiz,[†] Santiago Alvarez,*[,†] Roald Hoffmann,*[,‡] and Joel Bernstein[§]

Contribution from the Departament de Química Inorgànica, Universitat de Barcelona, Diagonal 647, 08028 Barcelona, Spain, Department of Chemistry, Cornell University, Ithaca, New York 14853, and Department of Chemistry, Ben Gurion University of the Negev, Beer-Sheva, Israel

Received November 26, 1993. Revised Manuscript Received May 25, 1994[⊕]

Abstract: A *crystal orbital displacement* function (COD) is defined as the variation of the contribution of an atomic orbital (or atom, fragment, or fragment molecular orbital) to the density of states (DOS) on going from a sublattice to the complete crystal lattice, within the one-electron approximation of tight-binding band calculations. This simple definition allows one to abstract relevant information on weak interactions in solids, by discarding the large amount of noninteracting levels and the strong (covalent or metallic) interactions present in complex systems. The degree of charge transfer between donor and acceptor sublattices can be obtained as the integral of a COD function (ICOD) up to the Fermi level, $\Omega_i(\epsilon_F)$. The general shapes of the COD curves are described, and simple examples of interpretation of the COD and ICOD diagrams to well-known chemical systems are presented. Extended Hückel tight binding (EHTB) band calculations and the derived COD and ICOD curves are applied to the study of host–guest interaction in the Hofmann clathrate $Ni(NH_3)_2Ni(CN)_4 \cdot 2C_6H_6$, and the role of the different building blocks of the host lattice in the host···guest interaction is discussed. The calculated barrier for the rotation of benzene around the molecular 6-fold axis, the predicted orientations of the guest molecules, changes in bond distances of the host and guest sublattices produced by enclathration, and variations of vibrational frequencies produced by enclathration are in agreement with a wealth of experimental data.

Inclusion compounds are in general formed by a host lattice with voids or tunnels in which guest molecules are enclathrated. The host···guest interactions may vary from charge-transfer forces to weak van der Waals interactions to hydrogen bonds.[1] One of the best known families of inclusion compounds is that of the Hofmann clathrates and their analogues.[2] The prototype of this family was prepared in 1897 by Hofmann and Küspert,[3-5] with the formula $Ni(CN)_2 \cdot NH_3 \cdot C_6H_6$ ($P4/m$, $a = 7.242$ Å, $c = 8.277$ Å, $Z = 2$). Generally speaking, the Hofmann clathrates correspond to the formula[6,7] $M(NH_3)_2M'(CN)_4 \cdot 2G$, with M = Mn, Fe, Co, Ni, Cu, Zn, or Cd; M′ = Ni, Pd, or Pt, and G = benzene, pyrrole, thiophene, dioxane, aniline, or biphenyl.[8] A related family of clathrates is obtained by substituting M′ by a metal ion with tetrahedral coordination (M′ = Cd, Hg).[9,10]

The goal of the work presented here is to analyze the host···guest interactions at the orbital level by using extended Hückel tight binding (EHTB) calculations. Such a study is expected to provide simple explanations for the effects of enclathration on the structural and spectroscopic parameters of the host lattice and the guest molecules. In addition, this case constitutes a rather stringent test for the ability of a one-electron model to provide information on the nature of weak interactions in inclusion compounds. Before going into the study of the Hofmann clathrates, we will define the crystal orbital displacement functions (COD) as a tool to simplify the analysis of the changes produced in the density of states (DOS) on going from a sublattice to the complete crystal lattice. The general shapes of the COD curves will be described, and two illustrative examples of application to well-known chemical systems are presented. With this tool at hand, we will briefly outline the main structural, chemical, and spectroscopic properties of the Hofmann clathrates, describe the electronic structure of the host lattice $Ni(NH_3)_2Ni(CN)_4$, and then examine its interactions with the benzene guest molecule. Similar studies with pyrrole and aniline as guest molecules and on a clathrate formed by an ethylenediamine-containing host lattice and benzene will be reported elsewhere.[11] The tetrahedral host lattice $Cd(CN)_2$ and its interaction with nonaromatic molecules will also be reported.[12]

Crystal Orbital Displacement Functions

The most common way to represent the electronic structure of a compound in the solid state is through its density of states (DOS) plot,[13] in which the number of one-electron states are given as a function of the energy, $n(\epsilon)$. From the total DOS, one can easily project the contributions of specific atoms or orbitals, therefore achieving a good degree of understanding of the orbital nature and atomic localization of the different regions of the DOS map.[14,15] In addition, crystal orbital overlap population

† Universitat de Barcelona.
‡ Cornell University.
§ Ben Gurion University of the Negev.
⊕ Abstract published in *Advance ACS Abstracts*, August 1, 1994.
(1) Zubkus, V. E.; Tornau, E. E.; Belosludov, V. R. In *Advances in Chemical Physics*; I. Prigogine, I., Rice, S. A., Eds.; John Wiley & Sons: New York, 1992; Vol. 81, pp 269–359.
(2) Iwamoto, T. In *Inclusion Compounds*; Atwood, J. L., Davies, J. E. D., MacNicol, D. D., Eds.; Academic Press: London, 1984; Vol. 1, pp 29–57.
(3) Hofmann, K. A.; Küspert, F. Z. *Z. Anorg. Chem.* **1897**, *15*, 204–207.
(4) Hofmann, K. A.; Höchtlen, F. *Chem. Ber.* **1903**, *36*, 1149–1151.
(5) Hofmann, K. A.; Arnoldi, H. *Chem. Ber.* **1906**, *39*, 339–344.
(6) Iwamoto, T. *Isr. J. Chem.* **1979**, *18*, 240–245.
(7) Iwamoto, T. *J. Mol. Struct.* **1981**, *75*, 51–65.
(8) Iwamoto, T.; Miyoshi, T.; Sasaki, Y. *Acta Crystallogr.* **1974**, *B30*, 292–295.
(9) Kiyoki, M.; Iwamoto, T.; Ohtsu, Y.; Takeshige-Kato, Y. *Bull. Chem. Soc. Jpn.* **1978**, *51*, 488–491.
(10) Kuroda, R. *Inorg. Nucl. Chem. Lett.* **1973**, *9*, 13–18.
(11) Ruiz, E.; Alvarez, S. To be published.
(12) Ruiz, E.; Alvarez, S. To be published.
(13) Ashcroft, N. W.; Mermin, N. D. *Solid State Physics*; Saunders: Philadelphia, 1976.
(14) Hoffmann, R. *Solids and Surfaces. A Chemist's View of Bonding in Extended Structures*; VCH: New York, 1988.
(15) Cox, P. A. *The Electronic Structure and Chemistry of Solids*; Oxford University Press: Oxford, 1987.

0002-7863/94/1516-8207$04.50/0

(COOP) plots[16] provide information on the bonding or antibonding characteristics of the different energy levels. There is a well-established methodology for ab initio calculations of semiconductors and insulators within the Hartree–Fock formalism,[17] but its application is nowadays limited to crystals with high symmetry and relatively small unit cells, and the one-electron DOS plots are still a reasonable approximation for a large number of problems of chemical interest.

When faced with the analysis of weak interactions in the solid state, such as ionic bonds or host···guest interactions in clathrates, the relevant information on such interactions is buried in the DOS and COOP curves under the wealth of information corresponding to the stronger and more abundant interactions between covalently (or metallic) bonded atoms. It would therefore be highly useful to dispose in some way of the large amount of irrelevant information. What is needed is just to describe a solid S as formed by two weakly interacting sublattices, A and B, and look at the variations of the DOS of one of those sublattices (or of its projections) when combined with each other. Let us define such variations as crystal orbital displacement functions (abbreviated COD from here on):

$$\Delta_i^A(\epsilon) = n_i^S(\epsilon) - n_i^A(\epsilon) \quad (1)$$

where $n_i^S(\epsilon)$ is the ith contribution to the DOS of the solid S and $n_i^A(\epsilon)$ is the ith contribution to the DOS of the sublattice A with energy ϵ. The units for the COD functions are the number of displaced levels per unit cell for the corresponding differential of energy. A variety of COD functions can be defined depending on the DOS contributions (i) analyzed, be they from atomic orbitals or atoms in the unit cell, or even from sets of atoms or orbitals (i.e., fragments or fragment orbitals). Similar COD functions can also be defined for the alternative sublattice B.

For the COD functions to be significant, the contributions to the DOS must be normalized according to eq 2,

$$\int_{-\infty}^{+\infty} n_i^S(\epsilon)\, d\epsilon = \int_{-\infty}^{+\infty} n_i^A(\epsilon)\, d\epsilon = N \quad (2)$$

where N is the total number of orbitals per unit cell included in the ith contribution. It follows that the COD functions have the following properties:

$$\lim_{E\to\infty} [\int_{-\infty}^{E} \Delta_i(\epsilon) d\epsilon] = 0 \quad (3)$$

$$\Delta_i(+\infty) = \Delta_i(-\infty) = 0 \quad (4)$$

In order to foresee the shapes to be expected for COD functions as well as their meaning, let us consider first a hypothetical solid formed by two interacting sublattices: a sublattice A, with one filled electronic band, and a sublattice B, having only one empty band (Figure 1). Upon interaction, the A-filled band is stabilized and some B levels are mixed into it, whereas the empty B band is destabilized, incorporating some levels from sublattice A.

If we now define a COD function for sublattice A, it should have roughly the aspect of Figure 1 (COD A): at low energy, a positive peak indicates the presence of some levels of A in the solid which do not appear at the same energy for the isolated sublattice. Conversely, the negative peak at slightly higher energy detects the absence of levels in the solid which were present in the sublattice. The presence of both positive and negative peaks at similar energies is the translation to the COD diagram of the band stabilization. Finally, a small peak at higher energies corresponds to the appearance of some levels of A mixed into the empty band. A similar analysis relates the COD diagram of sublattice B to the schematic band interaction diagram (Figure 1).

(16) Hughbanks, T.; Hoffmann, R. *J. Am. Chem. Soc.* **1983**, *105*, 3528.
(17) Pisani, C.; Dovesi, R.; Roetti, C. *Hartree-Fock Ab Initio Treatment of Crystalline Systems*; Springer Verlag: Berlin, 1988.

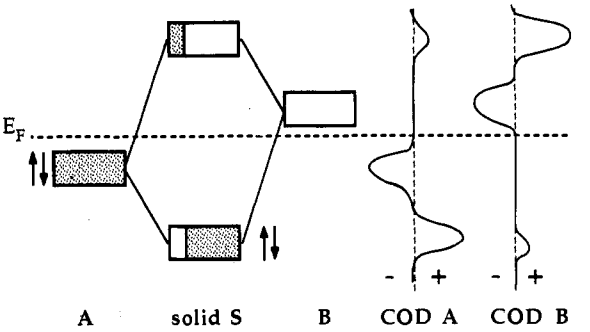

Figure 1. Block diagram for the interaction between the occupied band of a sublatice A and the empty band of a sublattice B. The shaded areas in the band blocks of the solid S represent the participation of the orbitals of sublattice A, and the white areas the participation of the orbitals of sublattice B. The corresponding COD curves for the levels of each sublattice are schematically shown at the right-hand side. E_F represents the Fermi level.

An interesting piece of information provided by the COD diagrams is the degree of charge transfer in a donor–acceptor interaction. In the scheme of Figure 1, sublattice A is acting as a donor toward sublattice B, and the amount of electron density donated is given by the number of B levels participating in the occupied band of the solid, i.e., by the intensity of the small peak below the Fermi level in the COD curve of B. In the general case, with more than one band per sublattice, the degree of charge transfer can be obtained by integrating the COD function up to the Fermi level. In the sequel it will be useful to define the value of that integral for a given energy. The new functions, abbreviated ICOD and represented by $\Omega_i(E)$, are defined as in eq 5:

$$\Omega_i(E) = \int_{-\infty}^{E} \Delta_i(\epsilon)\, d\epsilon \quad (5)$$

Note that the value of the ICOD function at the Fermi level for a particular orbital, atom, molecular fragment, or sublattice, $\Omega_i(\epsilon_F)$, represents its gain in electron density upon interaction with another sublattice to form the crystal.

After introducing the simple concept of COD and ICOD functions, we attempt a systematic description of the features to be expected in such diagrams and how they relate to the interaction between bands of different sublattices. Let us focus on a particular band of a sublattice. The perturbing effect of another sublattice in the real solid may in principle have three different effects on teh band under consideration: (1) net stabilization (or destabilization) of the band; (2) mixing in of orbitals from the perturbing sublattice, and (3) changes in its bandwidth. Although these effects appear combined in real cases, it is worthwhile to analyze them separately first. Such simplified examples are sketched out in Scheme 1. The first case to consider is the rigid stabilization (or destabilization) of a band represented in **1a** (**1b**), in which all levels within the band are shifted in energy by the same amount. The appearance of levels in the solid at lower energy than in the sublattice is reflected by a positive peak in the COD curve, whereas the absence of levels at the energies corresponding to the band in the sublattice gives place to a negative peak. The difference in energy between the negative and positive peaks is a measure of the stabilization of the band (i.e., the strength of the stabilizing interaction). The same magnitude is also reflected in the width of the corresponding ICOD peak. Notice that, if the stabilized band is full, the ICOD diagram reaches the zero line at energies below the Fermi level. The reader can easily check that the COD and ICOD curves for band destabilization present similar patterns with the peaks inverted (**1b**).

The second hypothetical case is that of orbital mixing without changes in the energies of the band levels. The levels centered in sublattice A are represented in the block diagram of **2a** and **2b** by shaded areas, and the levels centered at sublattice B by white areas. Mixing in of some B levels into the band of sublattice A is reflected in the COD diagram of B as a small positive peak

Scheme 1

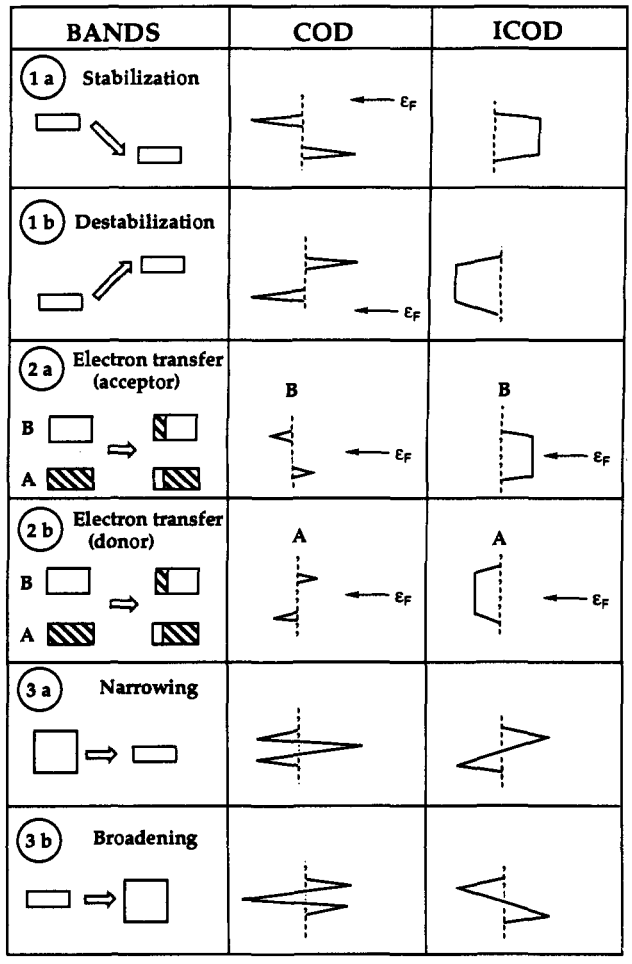

in the corresponding energy region. Consequently, the number of B levels in the "B" band is decreased, and a small negative peak appears in the energy region of that band. If the band of sublattice A is filled and that of B is empty, the outcome of band mixing is a transfer of electron density from A to B. The actual amount of charge transfer is given by the value of the ICOD function at the Fermi level, being positive for the acceptor and negative for the donor sublattice. Let us stress that, despite the analogous patterns of plots **1a** and **2a**, the two cases can be unequivocally identified thanks to (i) the smaller peaks in **2a** and (ii) their position relative to the Fermi level. The width of the ICOD peak in this case measures the energy difference between the two interacting bands. Let us remark that the interpretation of the value of the ICOD function at the Fermi level as a measure of the charge transfer between sublattices can be applied only when there is no change in the occupation but only in the composition of the bands on going from the sublattices to the full solid.

Finally, a narrowing (or broadening) of a band would produce characteristic W patterns in the COD diagrams, illustrated in **3a** (**3b**), akin to second derivative plots. One must be aware, however, that changes in bandwidths may be an artifact of the fitting procedure of the DOS and can be avoided by using a finer mesh of k-points in the calculations (see next section).

Before proceeding to the study of the electronic structure of the Hofmann clathrate and to the analysis of the host···guest interactions therein, we present in the following sections two examples of application of the COD and ICOD diagrams to different chemical aspects of well-known systems: (a) weak (ionic) interactions between the cationic and anionic sublattices of NaCl and (b) the Peierls distortion in polyacetylene.

Ionic Interaction in NaCl

Sodium chloride has been chosen as a first example because of its structural simplicity (one atom per unit cell in each sublattice), high symmetry, and high ionic character. Although the simplicity of the system would allow us to analyze band interactions without the use of COD diagrams, it is this simplicity which makes it a good introductory example, since we will be able to detect the interactions in the projections of the DOS and compare with the COD curves. The latter aspect, the highly ionic character of bonding in NaCl, provides a good test of the ability of the COD formalism to detect the weak orbital interactions existing in an ionic solid.

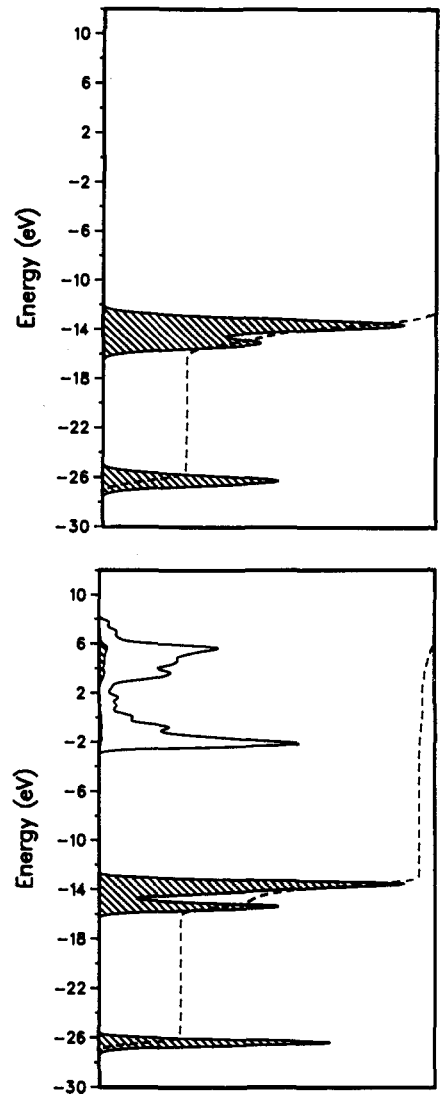

Figure 2. Density of states of the Cl atomic 3s and 3p orbitals in the sublattice of chlorides (top) and in the NaCl lattice (bottom), obtained with a set of 20 k-points.

The contributions of the Cl atoms to the DOS of NaCl and of the chloride sublattice are shown in Figure 2. Only small changes appear upon interaction with the sodium sublattice, as deduced by comparing both diagrams: (i) a narrowing of the lowest occupied band; (ii) a larger splitting of the second band, apparently associated with changes in the bandwidths and relative intensities of its subbands; (iii) a small contribution of the Cl atoms to the empty band at higher energy, formally a sodium band.

Substracting the two DOS diagrams yields the COD curve shown in Figure 3. The presence of peaks in the COD diagram detects the existence of interaction between the anionic and cationic sublattices. The peak in the region of the Cl 3s band (at *ca.* −26 eV) indicates the simultaneous stabilization and narrowing of that band through interaction with the Na^+ ions. A similar behavior is found for the Cl 3p bands: each 3p subband is narrower

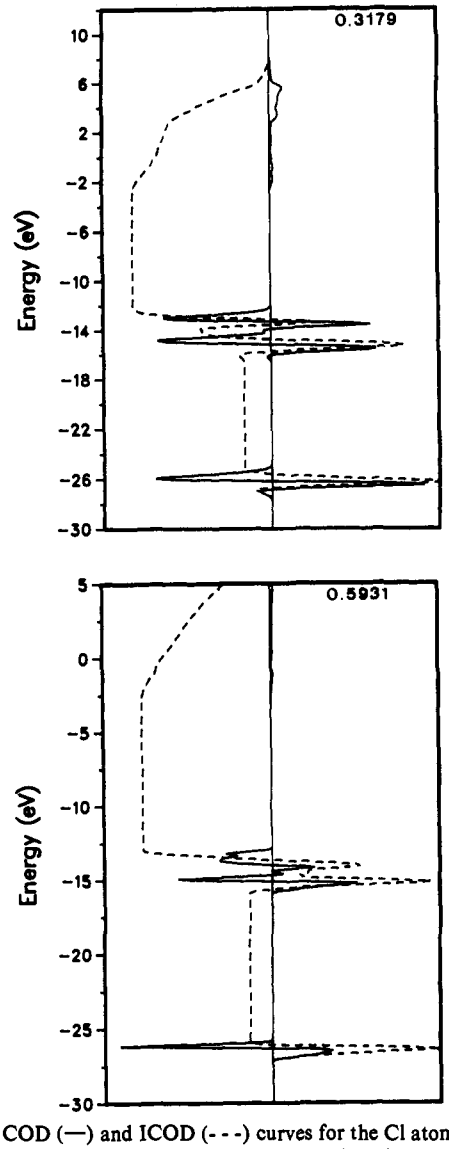

Figure 3. COD (—) and ICOD (- - -) curves for the Cl atomic orbitals in NaCl obtained with a set of 20 k-points (top) and with 84 k-points (bottom). The full scale for the COD curve corresponds to the number indicated in the upper right corner in units of number of displaced levels per unit cell.

and more stable after interaction with the Na^+ sublattice. A careful examination of the band energies reveals that, in contrast with the indication of the DOS and COD curves, the calculated bandwidths are practically invariant on going from the sublattice to the full solid. In fact, it is the fitting of the DOS curves which makes these bands appear narrower in the NaCl crystal than in the sublattice. This artifact can be avoided by increasing the size of the set of k-points used to calculate the DOS. In Figure 3 we compare the COD curve obtained with a set of 20 k-points and that calculated with a larger set (84 k-points). The former shows the W pattern expected for band narrowing in the region of, for example, the Cl 3s band, which is no longer present in the second case.

The positive peak in the COD curve of Cl^- above the Fermi level shows that some chloride levels which are occupied in the Cl^- sublattice (i.e., in a purely ionic model) become empty in NaCl. The charge transfer goes mainly to the sodium p orbitals (between 2 and 6 eV).

Let us focus now on the integrated COD function of chloride (dashed line in Figure 3). Above the Cl 3s band, the ICOD function remains negative, meaning that some of the Cl 3s Bloch orbitals are displaced to higher energy in NaCl; that is, they participate in the empty sodium bands. The same effect, enhanced, appears for the Cl 3p bands, indicating that the 3p orbitals of Cl are more important for the Na···Cl interaction than 3s. The actual value of the Cl → Na charge transfer calculated as twice the value of the ICOD function at the Fermi level, $\Omega(\epsilon_F)$, is 0.30 electrons per atom, a relatively small value as should be expected for such ionic interaction. Let us recall that the amount of band stabilization is given by the width of the ICOD peaks. In this case, these peaks are quite narrow, the band levels being only slightly stabilized by ionic interactions.

In summary, NaCl provides an example of relatively simple COD and ICOD diagrams in which two expected effects (stabilization and mixing) appear simultaneously and can be easily understood by comparison with the ideal cases sketched in Scheme 1. The apparent narrowing of bands is seen to be an artifact which can be avoided by using a finer mesh of the Brillouin zone.

Peierls Distortion in Polyacetylene

The use of COD and ICOD functions is not limited to the study of interactions between two sublattices; structural distortions can also be handled in this way. Let us consider as an example the bond alternation in the one-dimensional chains of polyacetylene. Such pairing distortion, due to a Peierls effect[18] can be easily detected by plotting the one-dimensional band structure before and after the distortion,[19] and there is in principle no need for an analysis of its COD functions. However, we will show in this section that the COD functions provide additional insight into the orbital nature of Peierls distortions. In general, whenever a Peierls distortion brings about a metal–semiconductor transition, the generation of a gap should be clearly detectable in the simpler and cheaper calculation of the band dispersion diagram. However, if one wants to explore the possibility of electronically driven structural distortions accompanying metal-to-metal transitions, the electronic effect may not be appreciated in the dispersion diagrams or the DOS plots, and the use of COD functions might be helpful.

In this case, the COD function for the ith orbital is defined as

$$\Delta_i(\epsilon) = n_i^D(\epsilon) - n_i^R(\epsilon) \qquad (6)$$

where $n_i^R(\epsilon)$ is the ith contribution to the DOS of the regular structure and $n_i^D(\epsilon)$ is the ith contribution to the DOS of the distorted structure. For the case of polyacetylene, we take first an *ideal* chain with all C—C distances the same (**4**) and then a *distorted* chain in which single and double C—C bonds alternate (**5**). Since we already know that the stabilization achieved through

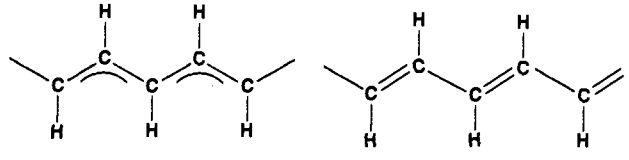

4 **5**

this distortion is associated with the partially filled π bands, it is enough to analyze COD diagrams for the contributions of these orbitals to the DOS of the ideal and the distorted chains. The contributions of the π-type orbitals to the DOS of the ideal and distorted chains are shown in Figure 4. A gap at *ca.* −11 eV in the DOS of the distorted structure is indicative of a stabilization of the levels lying just below the Fermi level and a destabilization of those lying just above it.

By substracting the π contributions to the DOS of both structures, the COD plot of Figure 5 is obtained. Notice that the most intense negative peak in the COD curve corresponds exactly to the gap in the distorted structure; that is, all levels around the Fermi energy have been displaced as a result of the structural

(18) Peierls, R. E. *Quantum Theory of Solids*; Clarendon Press: Oxford, 1955; p 108.
(19) Whangbo, M.-H.; Hoffmann, R.; Woodward, R. B. *Proc. R. Soc. London, Ser. A* **1979**, *366*, 23.

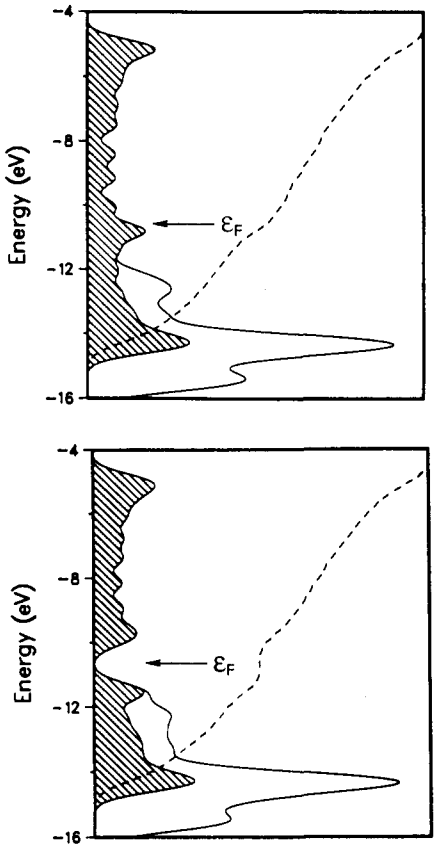

Figure 4. Total density of states of polyacetylene and contribution of the π orbitals (shaded area) in a regular (top) and a distorted (bottom) chain.

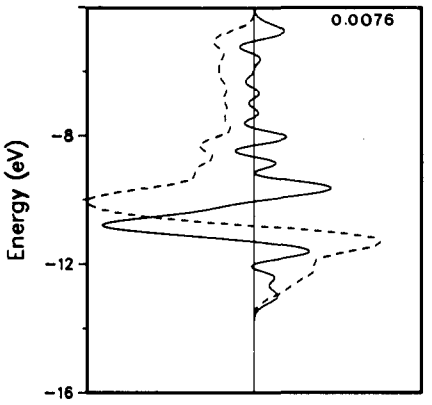

Figure 5. COD (—) and ICOD (- - -) curves for the π orbitals of polyacetylene. The COD curve is just the difference between the shaded areas of the two diagrams in Figure 4. The full scale for the COD curve corresponds to the number indicated in the upper right corner in units of number of displaced levels per unit cell.

distortion. Since there are positive peaks both below and above the gap, we can conclude that some levels have been stabilized and some have been destabilized. What is more interesting and has not been noticed previously is that not only does the distortion affect the band orbitals around the Fermi level but even the most bonding (positive peak at *ca.* −13 eV) and the most antibonding band levels (positive peak at *ca.* −4 eV) are shifted by the pairing distortion.

Crystal Structure and Properties of the Hofmann Clathrates

The lattice of the amminated nickel cyanide without enclathrated molecules consists of $[Ni(CN)_4]^{2-}$ square-planar units (we will refer to these nickel atoms as Ni_C in what follows). The nitrogen ends of the cyano groups are bound to another set of Ni atoms (labeled Ni_N hereafter), thus forming the layers shown in **6**. The coordination of the Ni_N atoms is completed by binding

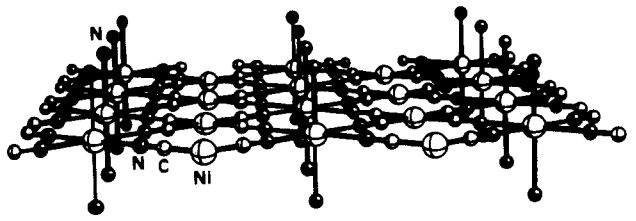

6

two NH_3 ligands in the axial positions. A top view of the square lattice of $Ni(CN)_2$ and a three-dimensional perspective of a $Ni(CN)_2(NH_3)$ layer are shown in Figure 6.

The relative position of adjacent layers of $Ni(CN)_2$ differs in the three known phases of $Ni(CN)_2 \cdot NH_3 \cdot xH_2O$ with varying degrees of hydration: in one phase the adjacent layers are eclipsed, while in the other two they are shifted. However, for the anhydrous compound, the most stable structure is the one in which the layers are shifted in such a way as to accommodate the axial ammonia ligands of one layer on top of the square-planar Ni_C metal atoms of the neighboring ones[20-22] (**7a**). An eclipsed layer stacking pattern (**7b**) can be obtained on substituting NH_3 by bridging ligands such as pyrazine or 4,4′-bipyridine.[23]

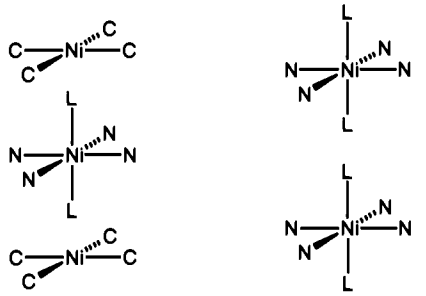

7a **7b**

The magnetic susceptibility of the host compound, $Ni(NH_3)_2Ni(CN)_4$, corresponds to one Ni atom in a square-planar and another one in a octahedral ligand field.[21] The thermal loss of the ammonia ligands produces a decrease in magnetic susceptibility and a change in the ν_{CN} infrared band, finally leading to $Ni(CN)_2$.[24,25]

The combination of the amminated nickel cyanide with an aromatic compound produces the Hofmann clathrates. In these, the layering pattern of the $Ni(CN)_2(NH_3)$ host sublattice is always eclipsed, except for the biphenyl clathrate: the axial ligands of one layer are aligned with those of the next layer (**7b**), and a molecule of, for example, benzene is incorporated as a guest inside the approximately cubic cavity defined by eight Ni atoms (Figure 6). The separation between layers clearly depends on the size of the guest molecule,[7] but some aromatic molecules are not enclathrated: toluene and xylene are examples of simple benzene derivatives which do not form Hofmann clathrates with the nickel–ammonia host lattice. The reason for this is not merely steric, since larger molecules such as biphenyl have been enclathrated.[8,26] The interlayer separation c, on the other hand, is not significantly

(20) Rayner, H. H.; Powell, H. M. *J. Chem. Soc.* **1958**, 3412.
(21) Ludi, A.; Hugi, R. *Helv. Chim. Acta* **1967**, *50*, 1283–1289.
(22) Mathey, Y.; Mazieres, C. *Can. J. Chem.* **1974**, *52*, 3637–3643.
(23) Mathey, Y.; Mazières, C.; Setton, R. *Inorg. Nucl. Chem. Lett.* **1977**, *13*, 1.
(24) Bose, D. M. *Nature* **1930**, *125*, 708.
(25) El-Sayed, M. F. A.; Sheline, R. K. *J. Inorg. Nucl. Chem.* **1958**, *6*, 187.
(26) Evans, R. F.; Ormrod, O.; Goalby, B. B.; Staveley, L. A. K. *J. Chem. Soc.* **1950**, 3346.

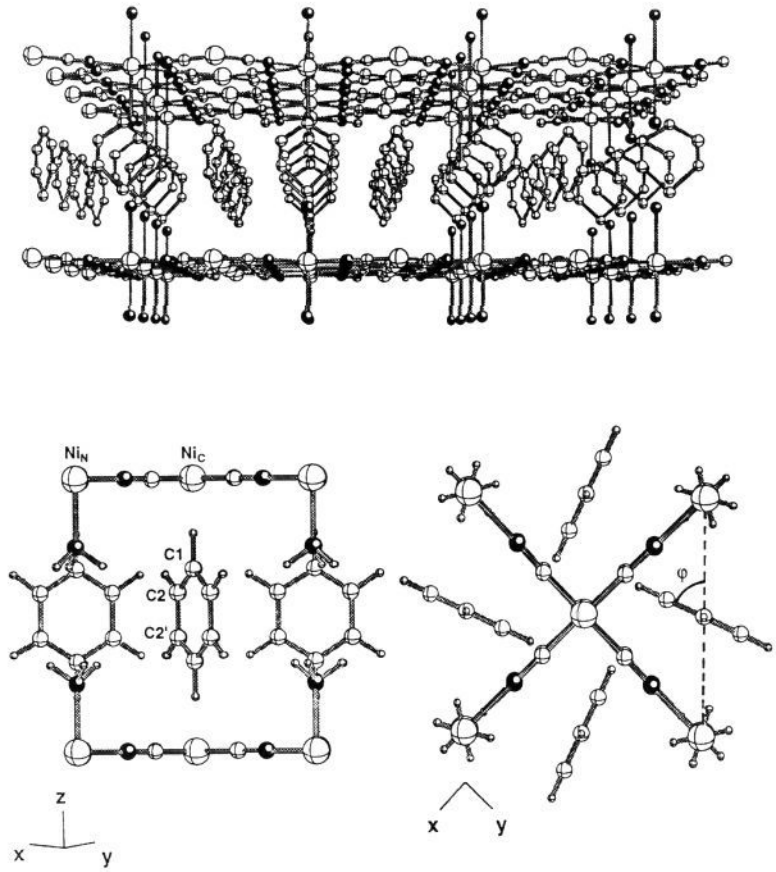

Figure 6. Perspective view of the structure of the Hofmann clathrates of the type $M(NH_3)_2M'(CN)_4{\cdot}2C_6H_6$. Black balls represent nitrogen atoms, large white balls nickel atoms, and small white balls carbon atoms.

altered by substituting Ni_C or Ni_N by metal atoms of different sizes.[8,26,27]

As far as the guest molecule is concerned, it is practiclaly always found in the middle of the interlayer cavities with a well-defined orientation. The benzene molecule, for instance, is always with a *para* axis parallel to the *c* crystallographic direction (Figure 6). The rotation of the guest molecules around this axis is hindered at low temperatures, and free rotation of benzene in the clathrate is only achieved above 160 K. This might be compared with molecular benzene crystals, in which free rotation is observed at 90 K.[28] The barrier to rotation of the guest within the host has been found to be 15.0–16.3 kJ/mol for the $Cd(NH_3)_2Ni(CN)_4{\cdot}2C_6H_6$ clathrate.[28,29]

The orientation of the guest molecules relative to the host sublattice is an interesting feature of these compounds. They are always found to deviate from the most symmetrical orientations ($\varphi = 0°$ or $\varphi = 90°$, Figure 6) and appear at angles $\varphi \approx 60°$ (Table 1). In such orientation, the plane of the guest molecule is pointing approximately toward the carbon atoms of the cyano groups. The fixed orientation of the benzene guest and its barrier for rotation about the axis perpendicular to the molecular plane suggest the existence of some sort of directional interaction between the guest molecules and the host sublattice. Only when L is a bulky ligand (ethylenediamine, en, or 2-aminoethanol, mea) is φ close to 90°, due probably to steric interactions (the volume occupied by such bulky axial ligands is schematically represented as the shaded region in a projection on the *ab* plane, **8**). Even when the host sublattice adopts a bent structure, with successive layers displaced with respect to each other due to severe steric constraints, the guest molecule is still oriented toward the cyano-C atoms.[30]

Some changes in M—C (–0.10 Å) and C—N (+0.07 Å) bond distances of the host lattice are observed upon enclathration.[20]

Table 1. Orientation of the Guest Molecules in Hofmann Clathrates of the Type $M(B)_2Ni(CN)_4{\cdot}2G$[a]

M	B	G	φ (deg)	ref
Ni	NH_3	C_6H_6	65.9	35, 36
Cd	NH_3	C_6H_6	58.5	35
Cd	NH_3	C_6H_6	67.7	39
Mn	NH_3	C_6H_6	66.5	35
Cu	NH_3	C_6H_6	64.3	38
Cd	*en*	C_6H_6	*85*	*41, 44*
Cd	en	C_4H_5N	90	45
Cd	NH_3	dioxane	46.3	31
Cd	mea	C_6H_6	90	24

[a] The orientation angle φ is defined in Figure 6.

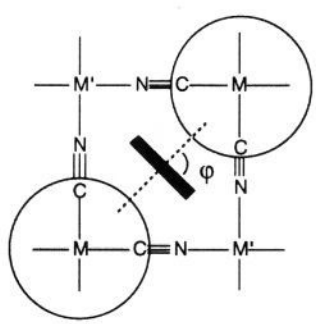

8

(27) Kuroda, R.; Sasaki, Y. *Acta Crystallogr.* **1974**, *B30*, 687–690.
(28) Miyamoto, T.; Iwamoto, T. *J. Mol. Spectrosc.* **1970**, *35*, 244–250.
(29) Ripmeester, J. A.; Ratcliffe, C. I. In *Spectroscopic and Computational Studies of Supramolecular Systems*; Davies, J. E. D., Kluwer Academic Publishers: Amsterdam, 1992; pp 1–27.
(30) Nishikiori, S.; Iwamoto, T. *Chem. Lett.* **1983**, 1129–1130.

Consistently, changes in the CN stretching frequencies (*ca.* −15 cm^{-1}) have also been reported. The vibrational spectra of the guest molecules are also affected by enclathration. In particular, the out-of-plane modes of benzene are shifted to higher frequencies relative to free benzene. This effect has been explained in terms of van der Waals interactions,[31,32] but it has also been suggested that the shifts are indicative of a weak hydrogen bond between NH_3 and the π system of benzene.[33]

Iwamoto and co-workers[34] have increased the number of families of inclusion compounds related to the Hofmann clathrates by substituting other amines for the ammonia groups. Typically, bidentate amines $NH_2(CH_2)_nNH_2$ (e.g., ethylenediamine, *en*) or hydroxylamines, such as monoethanolamine (*mea*),[30,35-37] have been employed as ligands, thus allowing one to fine-tune the interlayer distance and to modify the size of the cavities.[38,39] Although the most common guest molecules are aromatic compounds, clathrates of oxygen-containing molecules, such as dioxane[40] or 1-hexanol,[41] have been obtained. By using a host lattice of $Cd(CN)_2$, other nonaromatic molecules, such as neopentane[42] or halogenated derivatives of methane or ethane,[43] have been enclathrated.

Even if the host···guest interactions in clathrates are often assumed to be of the van der Waals type, thermodynamic studies[46,47] (DTA, DSC) indicate liberation energies of 50–60 kJ/mol. These energies are clearly higher than what one may expect for pure van der Waals interactions.[48] For a nonpolar molecule such as benzene, van der Waals interaction energies between induced dipoles of only 1–4 kJ/mol might be expected. In addition, van der Waals interactions are not highly directional and cannot account for the orientational preference of the guest molecules. Since the guest molecules are not very strongly bound to the host sublattice, thermal treatment may liberate guest molecules from the host lattice.[49,50]

By the judicious choice of M and L, a host lattice may be designed to allow for the selective enclathration of chosen molecules and its use, for example, in stationary phases for chromatography,[51] for the separation of different isomers of benzene derivatives,[52] or in the purification of benzene.[26,53,54] Oxidation reactions on the guest molecules, on the other hand, may lead to enclathrated conducting polymers, such as polypyrrole or polyaniline.[55]

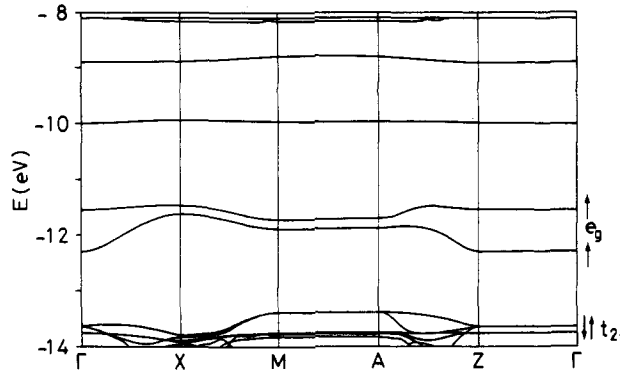

Figure 7. Band dispersion diagram of the host lattice $Ni(NH_3)_2Ni(CN)_4$ along several symmetry lines of the Brillouin zone.

Electronic Structure of the Host Lattice, $Ni(NH_3)_2Ni(CN)_4$

We recall that in this lattice there are two different types of Ni atoms. Ni_C is coordinated by the C atoms of four cyanide ligands in a square-planar geometry, whereas Ni_N is octahedrally coordinated by four N atoms of the cyanides and by two ammonia molecules.[56] Both types of Ni atoms are in the formal oxidation state +2. Usual ligand field or molecular orbital concepts provide us with a first approach to the electronic structure of the host lattice. Thus, the square-planar Ni_C atom is expected to have all its d electrons paired, whereas the octahedral Ni_N atom is expected to have a $t_{2g}^6e_g^2$ configuration, with two unpaired electrons. This description agrees well with the experimental magnetic moment of 3.2 μ_B[57] per repeat unit. On going from the local structure around the Ni atoms to the 2D layer, we expect the same qualitative description of the electronic structure, since through-space metal–metal interactions must be small.

In Figure 7 we show the band dispersion diagram calculated for the host lattice (see the Appendix for computational details). The two half-occupied bands built up from the e_g orbitals of Ni_N can be identified at −12.5 and −11.5 eV, respectively. The bands slightly below −13.5 eV are composed of the t_{2g} orbitals of the Ni_N atoms. The direct energy gap (ΓZ line of the Brillouin zone) between the t_{2g} and e_g levels, 10 *Dq*, corresponds to the energy of the first ligand field transition ($^4T_{2g} \leftarrow {}^4A_{2g}$).[58] The calculated 10-*Dq* value (1.4 eV or 10 995 cm^{-1}) is in excellent agreement with spectral data: since the N-bound cyanide appears in the spectrochemical series in a position close to that of ammonia,[59,60] the expected 10-*Dq* value for the NiN_6 chromophore should be close to that of $[Ni(NH_3)_6]^{2+}$ (10 750 cm^{-1}).[61]

As we will see later, the ligand field view of the electronic structure of the host lattice cannot account for the host···guest interactions in the Hofmann clathrates. A more detailed description of the composition of the electronic bands of the host lattice is needed. Hence, we analyze the contributions of the different groups to the density of states (DOS): CN^- (Figure 8a), NH_3 (Figure 8b), Ni_C (Figure 8c), and Ni_N (Figure 8d). The assignment of the different peaks of the density of states (DOS) has been carried out with the aid of the crystal orbital

(31) Bhatnagar, V. M. *Chim. Anal.* **1967**, *49*, 563.
(32) Miyoshi, T.; Iwamoto, T.; Sasaki, Y. *Inorg. Chim. Acta* **1967**, *1*, 120–126.
(33) Akyuz, S.; Dempster, A. B.; Morehouse, R. L. *Spectrochim. Acta* **1974**, *30A*, 1989–2004.
(34) Iwamoto, T. In *Inclusion Compounds*; Atwood, J. L., Davies, J. E. D., MacNicol, D., Eds.; Oxford University Press: Oxford, 1991; Vol. 5, pp 177–212.
(35) Nishikiori, S.; Iwamoto, T. *Bull. Chem. Soc. Jpn.* **1983**, *56*, 3246–3252.
(36) Nishikiori, S.; Iwamoto, T. *Chem. Lett.* **1984**, 319–322.
(37) Nishikiori, S.; Iwamoto, T. *Chem. Lett.* **1982**, 1035–1038.
(38) Hashimoto, M.; Hasegawa, T.; Ichida, H.; Iwamoto, T. *Chem. Lett.* **1989**, 1387–1390.
(39) Hashimoto, M.; Iwamoto, T. *Chem. Lett.* **1990**, 1531–1534.
(40) Kendi, E.; Ulku, D. *Z. Kristallogr.* **1976**, *144*, 91–96.
(41) Hasegawa, T.; Iwamoto, T. *J. Incl. Phenom.* **1988**, *6*, 143.
(42) Kitazawa, T.; Nishikiori, S.; Yamagishi, A.; Kuroda, R.; Iwamoto, T. *J. Chem. Soc., Chem. Commun.* **1992**, 413–415.
(43) Kitazawa, T.; Nishikiori, S.; Kuroda, R.; Iwamoto, T. *Chem. Lett.* **1988**, 1729–1732.
(44) Miyoshi, T.; Iwamoto, T.; Sasaki, Y. *Inorg. Chim. Acta* **1972**, *7*, 97–101.
(45) Sasaki, Y. *Bull. Chem. Soc. Jpn.* **1967**, *42*, 2412.
(46) Ohyama, J.; Tsuchiya, R.; Uehara, A.; Kyuno, E. *Bull. Chem. Soc. Jpn.* **1977**, *50*, 410.
(47) Uemasu, I.; Iwamoto, T. *Chem. Lett.* **1982**, 973.
(48) Pauling, L. *The Nature of the Chemical Bond*, 3rd. ed.; Cornell University Press: Ithaca, 1960.
(49) Sopková, A. *Proc. Termanal.* **1973**, *73A*, 77.
(50) Sopková, A.; Bubanec, J. *J. Therm. Anal.* **1977**, *12*, 97.
(51) Sopková, A.; Singliar, M. In *Inclusion Compounds*; Atwood, J. L., Davies, J. E. D., MacNicol, D. D., Eds.; Academic Press: London, 1984; Vol. 3.
(52) Davies, J. E. D.; Maver, A. M. *J. Mol. Struct.* **1983**, *102*, 203.
(53) Jones, A. L.; Fay, P. S. U.S. Patent 2,732,413, 1958.
(54) Sopková, A.; Singliar, M.; Bubanec, J.; Gornerova, T.; Kralik, P. Czech. Patent 222,610,9, 1983.
(55) Kanatzidis, M. G.; Wu, C.-G.; Marcy, H. O.; DeGroot, D. C.; Schindler, J. L.; Kannewurf, C. R.; Benz, M.; LeGoff, E. In *Supramolecular Architecture. Synthetic Control in Thin Films and Solids*; Bein, T., Ed.; *ACS Symp. Ser.* 499; American Chemical Society: Washington, DC, 1992; p 194.
(56) Rae, A. I. M.; Maslen, E. N. *Z. Kristallogr.* **1966**, *123*, 391–396.
(57) Iwamoto, T.; Nakano, T.; Morita, M.; Miyoshi, T.; Miyamoto, T.; Sasaki, Y. *Inorg. Chim. Acta* **1968**, *2*, 313–316.
(58) Ballhausen, C. J. *Introduction to Ligand Field Theory*; McGraw-Hill: New York, 1962; p 74.
(59) Alvarez, S.; López, C. *Inorg. Chim. Acta* **1982**, *64*, L99.
(60) Shriver, D. F.; Shriver, S. A.; Anderson, S. E. *Inorg. Chem.* **1965**, *4*, 725–730.
(61) Lever, A. P. B. *Inorganic Electronic Spectroscopy*, 2nd ed.; Elsevier: Amsterdam, 1984.

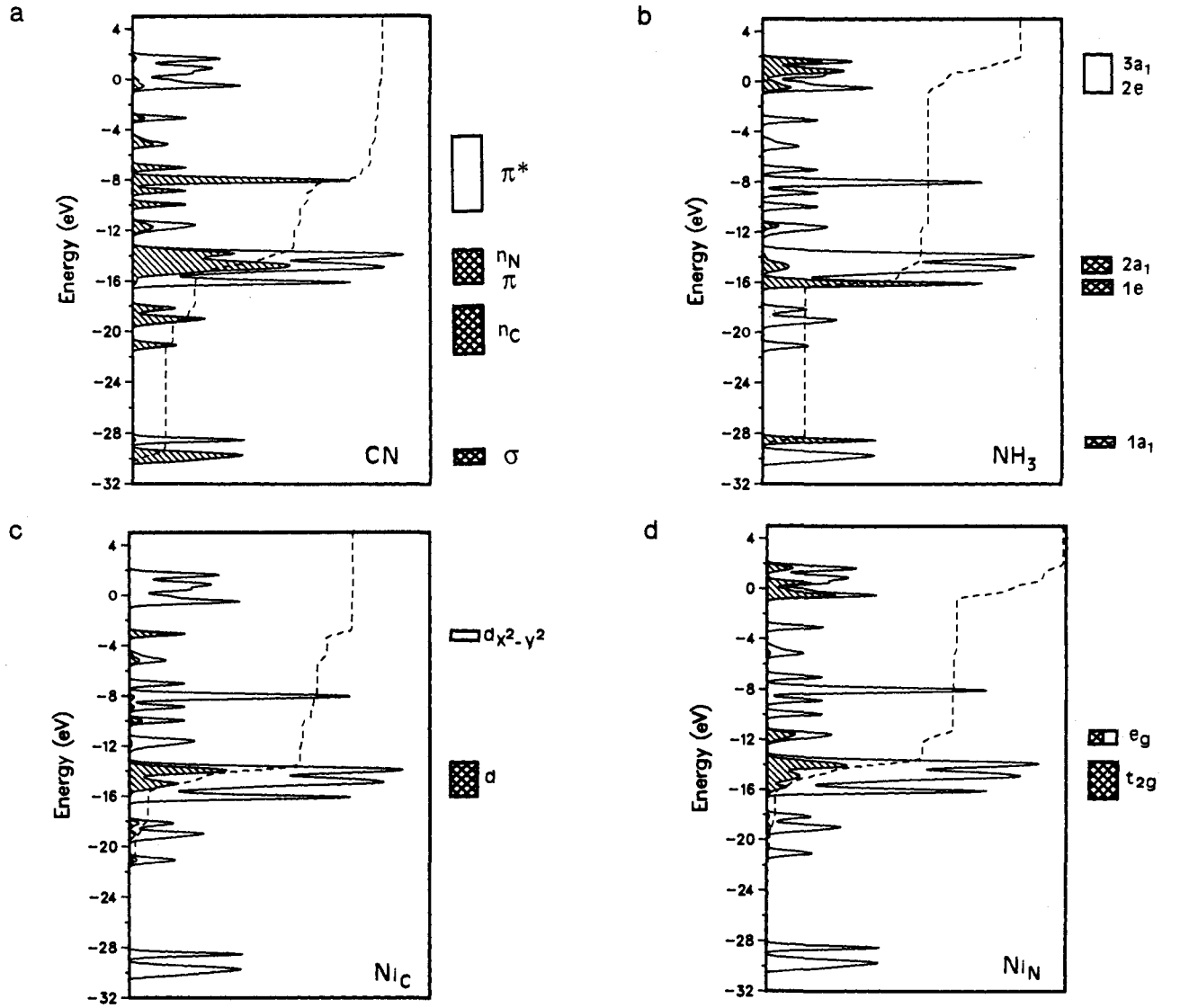

Figure 8. Density of states of the host lattice $Ni(NH_3)_2Ni(CN)_4$ and contributions of the cyano groups (CN), ammino ligands (NH_3), carbon-bound nickel atom (Ni_C), and nitrogen-bound nickel atom (Ni_N). The highest occupied band, at *ca.* −11 eV, is half-occupied. The blocks at the right-hand side of each DOS diagram are schematic representations of the band levels associated with each fragment.

overlap population (COOP) curves,[14,16] omitted here for simplicity. The energy window is now much wider than for Figure 7.

Let us make a brief description of the different contributions to the DOS of the host lattice, $Ni(NH_3)_2Ni(CN)_4$:

(a) CN (Figure 8a). The peaks between −22 and −18 eV (labeled n_{CN}) have nonbonding character and can be attributed to the cyanide lone pairs essentially localized on the C atoms and stabilized through interaction with Ni. These correspond, in increasing order or energies, to the symmetry-adapted combinations a_{1g}, e_g (double intensity), and b_{1g}. At energies between −16 and −13 eV, the π-bonding orbitals are interspersed with the nitrogen lone pairs. Above, a set of peaks between −11 and −6 eV correspond to bands generated by the eight π^* orbitals.

(b) NH_3 (Figure 8b). The N—H bonding orbitals a_1 and e appear as low-lying peaks (at −28 and −16 eV, respectively). The peak corresponding to the N lone pairs is split into two components (−15 and −11.5 eV) due to the interaction with d_{z^2} of Ni_N. In the energy range from −1 to 3 eV one finds the N—H antibonding orbitals: the lowest band is built up of the $3a_1$ orbitals of ammonia mixed with p_z of Ni (**9a**); at slightly higher energy is a band composed of the ammonia $2e^+$ orbitals (**9b**, participation of Ni orbitals in this band is forbidden by symmetry); and still higher is the band formed by the $2e^-$ combination with N—Ni antibonding character (**9c**).

(c) Ni_C (Figure 8c). The ligand-field-destabilized $d_{x^2-y^2}$ band appears at about −3 eV and the remaining d bands of Ni_C between −16 and −13 eV.

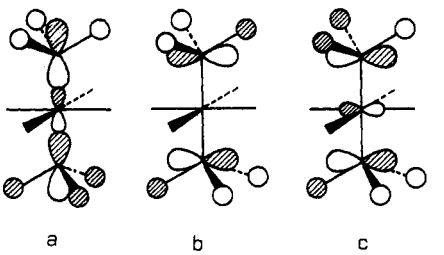

9

(d) Ni_N (Figure 8d). The contributions of this atom to the DOS can be assigned as follows: the t_{2g} levels appear between −16 and −13 eV, just below the half-occupied e_g bands (between −12.5 and −11.5 eV). The fact that the Ni_N d_{z^2} orbital appears at lower energy than $d_{x^2-y^2}$ of Ni_C is consistent with the relative position of ammonia and cyanide in the spectrochemical series. The three bands at high energies (−1 to 3 eV) correspond to the Ni—N antibonding orbitals, with contributions from the Ni 4p orbitals (**9a–c**).

Orientation of the Guest Molecule in the Hofmann Clathrate, $Ni(NH_3)_2Ni(CN)_4 \cdot 2C_6H_6$

Before analyzing the electronic structure of the clathrate of benzene and the host···guest interactions therein, we test the ability

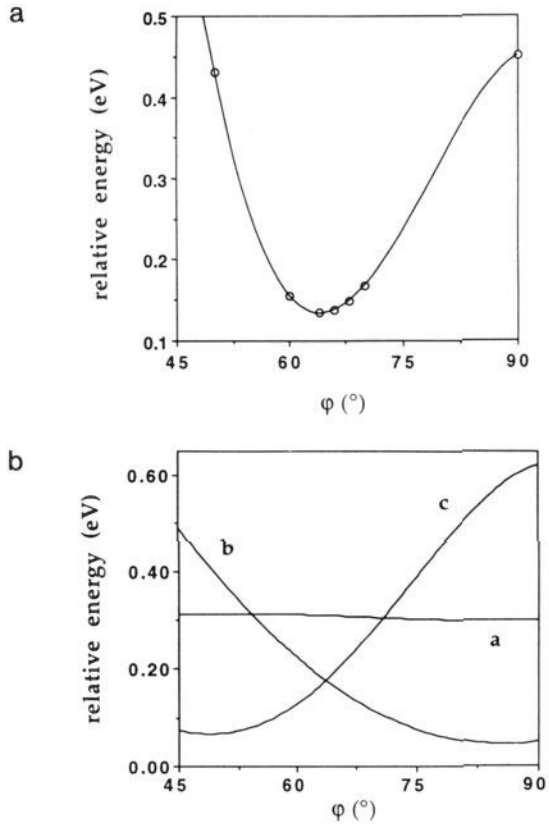

Figure 9. Total one-electron energy (top) of $Ni(NH_3)_2Ni(CN)_4 \cdot 2C_6H_6$ as a function of the rotation angle of benzene, φ (see **8**). Contributions to the one-electron energy are shown below: (a) benzene···$Ni_2(CN)_4$; (b) benzene···ammonia; and (c) benzene···benzene.

of our calculations to reproduce the conformational preference experimentally found for the guest molecule. For these calculations, the atomic coordinates based on the crystal structure determined by Rayner and Powell[62] were used. The molecule of benzene was allowed to rotate around the *c* axis. An energy minimum was found for a rotation angle $\varphi = 65°$ (Figure 9a), in excellent agreement with the experimental value of 65.9°.

The potential energy curve of Figure 9 can be decomposed into several contributions (see the Appendix for computational details): the interaction of benzene with the $Ni_2(CN)_4$ layers (curve a in Figure 9b) is virtually independent of the angle φ. Its interaction with the ammonia molecules (curve b, Figure 9b) favors the conformation with $\varphi = 90°$ (see Figure 6). Finally, interaction of a benzene molecule with the neighboring benzene molecules is strongly repulsive for the "star" arrangement (**10a**), corresponding to $\varphi = 90°$, and is favorable for the conformation $\varphi = 45°$, with mutually perpendicular benzene molecules (**10b**). Let us recall that geometry **10b** very closely approximates that found in solid benzene,[63] in which two neighboring molecules are practically perpendicular (90.4°), but shifted along the *c* axis. This relative arrangement of the benzene molecules has been theoretically studied by Hunter and Sanders,[64] who found the perpendicular arrangement to be more stable due to a σ–π attractive interaction, in contrast with the parallel and star conformations, found to be repulsive.

Therefore, it is the combined effect of the interactions of a benzene molecule with the axial ligands and with neighboring benzene molecules which determines the actual orientation of the guest molecule in the Hofmann clathrate studied. This result

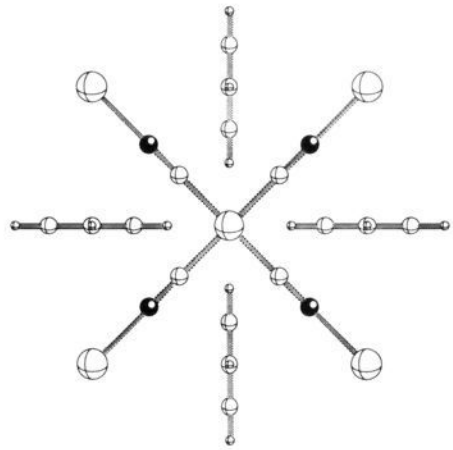

10a

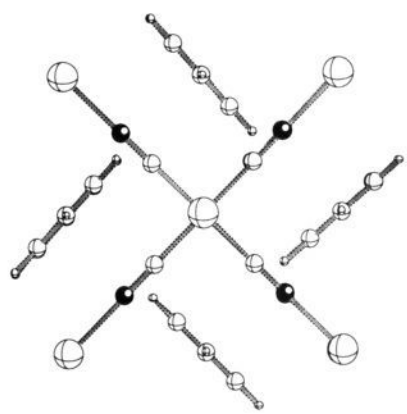

10b

is in agreement with the findings of Iwamoto *et al.* in MM2 molecular mechanics calculations[65] on bimolecular complexes NH_3/C_6H_6, C_6H_6/C_6H_6, and CN^-/C_6H_6.

Let us recall that the guest benzene molecule rotates at relatively low temperatures around the molecular 6-fold axis, with an estimated activation energy of 15.0–16.3 kJ/mol, according to the analysis of the ^1H- and ^2H-NMR line shapes[28,29] of $Cd(NH_3)_2Ni(CN)_4 \cdot 2C_6H_6$ and deuterated derivatives. Our calculated barrier for such a rotation of benzene is 16.2 kJ per mole of benzene, in excellent agreement with the experimental data.

Interaction of Benzene with the Host Lattice

In order to separate the interactions of a benzene molecule with the host lattice from those with the neighboring benzenes, we study now a model clathrate, $Ni(NH_3)_2Ni(CN)_4 \cdot C_6H_6$, in which only half of the cavities are occupied by benzene molecules. This leaves only benzene···benzene interactions between second nearest neighbors, which we assume to be negligible.

The contribution of the benzene molecules to the DOS of the clathrate $Ni(NH_3)_2Ni(CN)_4 \cdot 2C_6H_6$ is represented in Figure 10. The molecular orbitals of the isolated molecule are also shown for comparison. The contributions of benzene MOs to the DOS of the clathrate appear at practically the same energies as the molecular orbitals of the isolated molecule. Hence, one is tempted to conclude, by looking at Figure 10, that no significant interaction takes place between the guest molecule and the host lattice. But let us analyze the changes in the energy levels of benzene upon enclathration with the magnifying glass of the COD functions

(62) Rayner, H. H.; Powell, H. M. *J. Chem. Soc.* **1952**, 319–328.
(63) Cox, E. G.; Cruickshank, D. W. J.; Smith, J. A. S. *Proc. R. Soc.* **1958**, *247*, 1–21.
(64) Hunter, C. A.; Sanders, J. K. M. *J. Am. Chem. Soc.* **1990**, *112*, 5525–5534.
(65) Kitazawa, T.; Nishikiori, S.; Kuroda, R.; Iwamoto, T. *J. Incl. Phenom.* **1989**, *7*, 369–377.

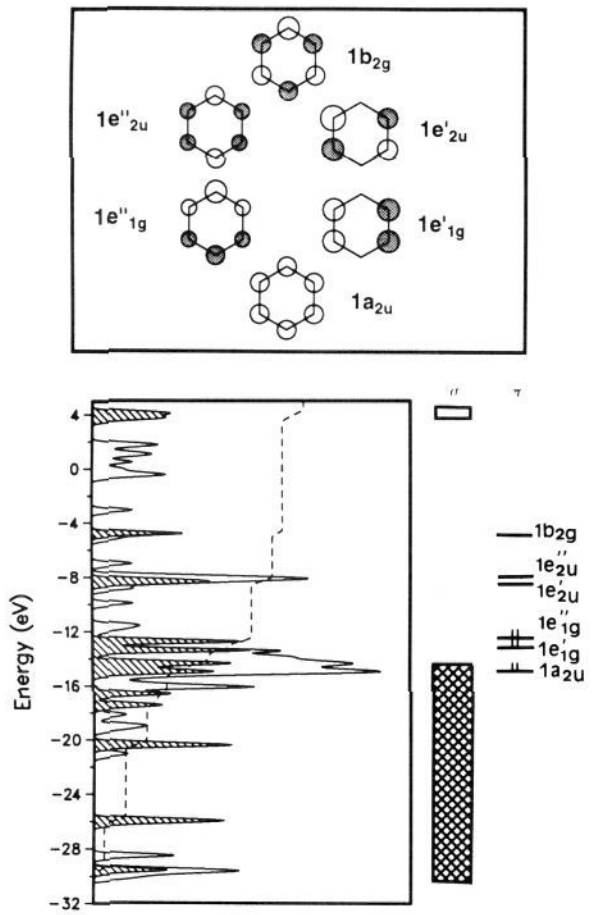

Figure 10. Molecular orbitals of benzene (top) and their contributions to the DOS of the Hofmann clathrate $Ni(NH_3)_2Ni(CN)_4{\cdot}2C_6H_6$ (bottom, shaded curve). The symmetry labels for benzene correspond to the idealized symmetric molecule (D_{6h} symmetry) and the orbitals of a degenerate pair are labeled, for example, e_{1g}' and e_{1g}''.

defined above. For a particular MO of benzene, the COD function is defined as

$$\Delta_i = n_i^C - n_i^G \tag{7}$$

where n_i^C is the contribution of the ith molecular orbital to the density of states of the clathrate and n_i^G its contribution to the DOS of the isolated guest molecules. Hence, the units for the COD functions are the number of displaced levels per unit cell for the corresponding differential of energy. For an occupied molecular orbital of the free guest molecule, the integral of its DOS up to the Fermi level is

$$\int_{-\infty}^{\epsilon_F} n_i^G \, d\epsilon = 1 \tag{8}$$

Mixing of an occupied MO of the guest molecule with empty levels of the host (guest to host charge transfer) results in a decrease of its integrated contribution to the DOS:

$$\int_{-\infty}^{\epsilon_F} n_i^C \, d\epsilon < 1 \tag{9}$$

As a result, the value of the ICOD function at the Fermi level is negative:

$$\Omega_i(\epsilon_F) = \int_{-\infty}^{\epsilon_F} (n_i^C - n_i^G) d\epsilon < 0 \tag{10}$$

On the other hand, mixing of an empty MO of the guest with occupied levels of the host (host to guest charge transfer) gives a positive value for the ICOD function at the Fermi level, $\Omega_i(\epsilon_F) > 0$. The calculated values for $\Omega_i(\epsilon_F)$ of several MOs of benzene are shown in Table 2.

Table 2. Calculated Values for the ICOD Functions of Molecular Orbitals of Benzene at the Fermi Level, $\Omega_i(\epsilon_F)$ ($\times 10^4$), in the Benzene Clathrate, $Ni(NH_3)_2Ni(CN)_4{\cdot}2C_6H_6$, in Increasing Order of Energy

Benzene Occupied Orbitals	
other σ orbitals [9][a]	−17
$1a_{2u}$ (π)	−19
$1b_{2u}$	−1
$3e_{2g}'$	−2
$3e_{2g}''$	−3
$1e_{1g}'$ (π)	−17
$1e_{1g}''$ (π)	−19
Benzene Empty Orbitals	
$1e_{2u}'$ (π^*)	6
$1e_{2u}''$ (π^*)	2
$1b_{2g}$ (π^*)	1
other σ^* orbitals [12]	22

[a] Number of orbitals given in brackets.

The numbers in Table 2 suggest that there is indeed some orbital interaction between benzene and the host, even if it is weak. The most important individual interactions correspond to electron density transfer from the occupied π orbitals of benzene, $1a_{2u}$ and $1e_{1g}$, to empty orbitals of the host lattice. Each individual interaction of σ-type orbitals is small, but the combined effect of all occupied σ orbitals of benzene is not negligible. The relevance of these numbers will be analyzed below. A quantitative assessment of the present results, obtained through ab initio calculations and reported elsewhere,[66] confirms all of the conclusions based on the semiempirical results presented here. Let us now analyze in more detail the COD and ICOD functions of several molecular orbitals.

Benzene π Orbitals. The COD curves of the occupied π orbitals of benzene (Figure 11) indicate that the interaction with the host lattice occurs mostly through the σ^*(N—H) orbitals of the NH_3 groups, $3a_1$ and 2e (**9a**, **9b**, and **9c**), in the high-energy region (0–3 eV). A smaller peak can also be seen between 24 and 28 eV due to the interaction of the benzene π orbitals with the strongly N—H antibonding $4a_1$ bands. Smaller contributions from the π^* orbitals of the cyano groups, below the energy windows of Figure 6, can also be detected. Not all the σ^*(N—H) orbitals participate to the same extent in the host···guest interaction, the more intense peaks being those of the $2e^+$ orbital at 2 eV (**9b**). Since the energy differences between the different occupied π orbitals of benzene and σ^*(N—H) of ammonia are similar, it is likely that the magnitude of the interaction is dictated by overlap. According to a perturbation analysis of orbital interactions, which can be appropriately applied to the weak host···guest interactions, the mixing coefficients depend on the overlap between the interacting orbitals.[67] The numbers shown in the COD curves (Figure 11) represent the overlap integrals ($\times 10^3$) between the corresponding π orbital of benzene and each of the σ^*(N—H) orbitals of the host lattice (**9a–c**), calculated for a nonperiodic model. The fact that the intensities of the COD peaks roughly follow the same trend as the overlap integrals indicates that the π(benzene)/σ^*(N—H) interaction is controlled by orbital overlap.

Benzene π^* Orbitals. Charge transfer from the occupied bands of the host lattice, coming predominantly from bonding orbitals of NH_3 ($2a_1$ and 1e), to the empty π^* orbitals of benzene is much smaller. As a result of the different participation of the various benzene π and π^* orbitals in charge transfer, the guest molecule loses its high symmetry, as discussed below.

Benzene σ and σ^* Orbitals. Although the most important host···guest interactions involve the π system of benzene, σ orbitals also contribute to such interactions (Table 2). From the analysis of the COD curves for the σ and σ^* orbitals of benzene (not shown here), one can conclude that the most relevant empty orbitals of the host lattice involved are π^*(CN) and again the $3a_1$

(66) Ruiz, E.; Novoa, J. J.; Alvarez, S. Submitted for publication.
(67) Albright, T. A.; Burdett, J. K.; Whangbo, M.-H. *Orbital Interactions in Chemistry*; J. Wiley: New York, 1984; p 29.

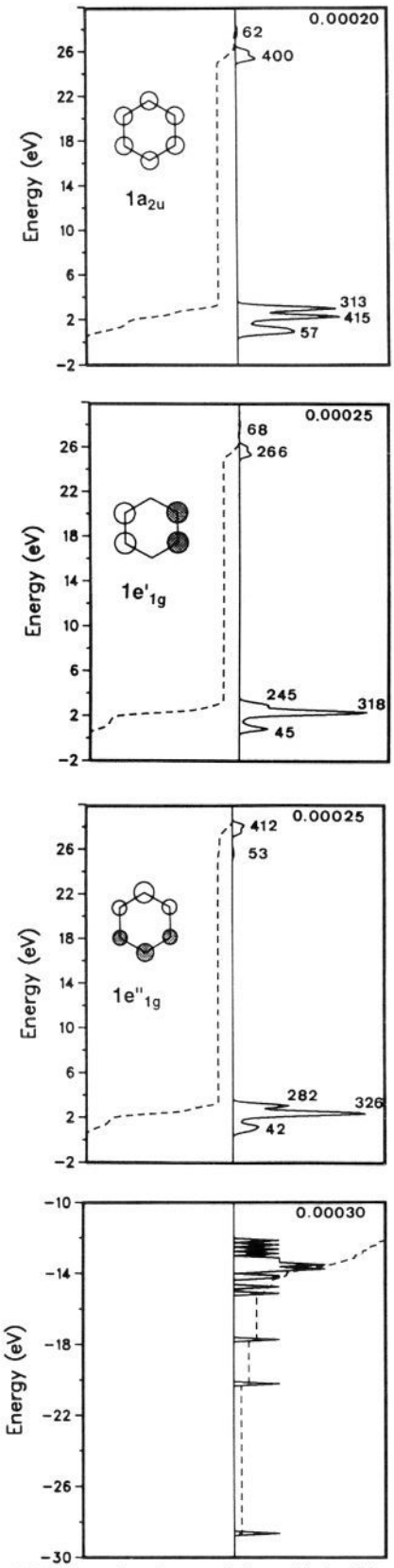

Figure 11. COD curves for the occupied π orbitals of benzene in the energy range of the empty orbitals ($1a_{2u}$ and the $1e_{1g}$ set) and for the σ^* orbitals of benzene in the energy range of the occupied orbitals of the host lattice. The full scale for the COD curve corresponds to the number indicated in the upper right corner in units of number of displaced levels per unit cell.

and 2e bands of NH_3. The empty σ^* orbitals of benzene accept electron density from the π orbitals and nitrogen lone pair orbitals of cyanide in the host lattice. The proximity of the hydrogen atoms of benzene to the nitrogen atoms of the cyanides suggests that this charge transfer could be considered as a hydrogen bond, as weak as might be expected for the H···NC distances in excess of 3 Å. Notice that such long distances do not preclude the existence of a hydrogen bond, according to the thorough analysis of the internuclear distance criterion of Jeffrey and Saenger.[68]

A calculation of the enclathration energy of a benzene molecule with a discrete molecular model at the INDO level[69] showed that the two main contributions come from the interaction of benzene molecules with NH_3 and, to a lesser extent, with the cyanides. The Ni atoms were not included in such calculations. These results are qualitatively consistent with those presented here, which are based on band calculations on the complete extended system. The different host···guest interactions described above and deduced from the analysis of the COD curves are schematically summarized in block form in **11a**. The orbital blocks shown can be identified in Figures 8 and 10.

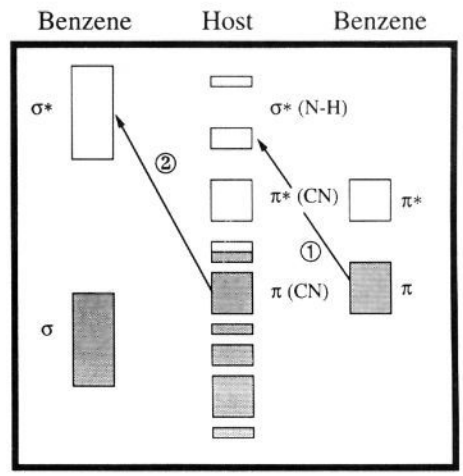

11a

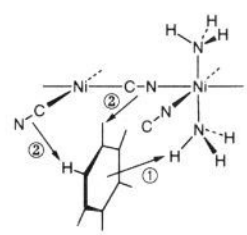

11b

Effect of Enclathration on the Charge Distribution. The electron densities most affected by enclathration are presented in Table 3. The electron occupation of the nitrogen atoms of the ammonia ligands increases upon enclathration. This electron density goes mainly to the p_x and p_y atomic orbitals, in agreement with the charge transfer to the 2e bands of ammonia discussed above. The carbon atoms of benzene lose electron density, mainly from the p_x and p_y atomic orbitals constituting the π system. It is worthy of note that in the CN groups it is the carbon rather than the nitrogen atoms which donate electron density, as imposed by the orientation of the benzene molecules relative to the cyanides (Figure 6).

A reexamination of the different contributions to the DOS in the Hofmann clathrate (Figure 8) shows that the $3a_1$ and $2e^-$ bands have important contributions from the Ni_N atoms, corresponding to their $\sigma^*(Ni—NH_3)$ character. Hence, the

(68) Jeffrey, G. A.; Saenger, W. *Hydrogen Bonding in Biological Structures*; Springer: Heidelberg, 1991; p 24–32.
(69) Uemasu, I. *Polyhedron* **1983**, *2*, 115–118.

Table 3. Atomic and Orbital Electron Populations Affected by Enclathration in the Hofmann Clathrate $Ni(NH_3)_2Ni(CN)_4{\cdot}2C_6H_6$

		host lattice	clathrate	difference
$N(NH_3)$	total	5.348	5.365	+0.017
	s	1.457	1.459	+0.002
	p_x	1.242	1.249	+0.007
	p_y	1.242	1.249	+0.007
	p_z	1.407	1.408	+0.001
C(CN)	total	3.386	3.381	−0.005
	p_z	0.656	0.653	−0.003
N(CN)	total	5.653	5.659	+0.006
	p_z	1.389	1.393	+0.004
		guest	clathrate	difference
C1		4.036	4.035	−0.001
H1		0.971	0.970	−0.001
C2		4.027	4.026	−0.001
H2		0.970	0.969	−0.001
C_6H_6		30.000	29.983	−0.017

calculated electron density at Ni_N increases by 0.004 due to interaction with the guest molecules. This result finds its experimental expression in the ^{113}Cd-NMR spectra[70] reported for the related clathrate $Cd(NH_3)_2Ni(CN)_4{\cdot}2C_6H_6$ and the corresponding isolated host, $Cd(NH_3)_2Ni(CN)_4$. An upfield shift of −50 ppm in the position of the Cd signal when benzene guest molecules are present clearly indicates an increase of the electron density at the octahedral metal atom.

Our interpretation is that the host···guest interactions are a particular type of *hydrogen bonds*[71,72] between benzene and ammonia (labeled 1 in **11**) and between cyanide and benzene (interactions of type 2 in **11**). The $H(NH_3)\cdots C(C_6H_6)$ overlap population is +0.0024, small but significant. Accordingly, the shortest H···C distances are approximately 2.6 Å (assuming the same N—H distance as in ammonia), clearly shorter than the van der Waals sum[48] (H, r_{vdW} = 1.2 Å; aromatic π system, r_{vdW} = 1.7 Å). Further, if the ammonia molecule is rotated (in the clathrate model with only one benzene molecule per unit cell), a minimum appears at a rotation angle coincident with the orientation found in INDO calculations on a bimolecular $NH_3\cdots C_6H_6$ complex.[69] Even if the variations in energy are small, they indicate the existence of an $NH_3\cdots C_6H_6$ interaction. These results have been confirmed through ab initio MP2 calculations on bimolecular complexes[66] and are consistent with the existence of numerous reports of C···HN, CH···N, and CH···O hydrogen bonds (see discussion below).

Is it reasonable to rely on the very small variations in the calculated electron densities for the interpretation of the host···guest interactions? There is some precedent in extended Hückel MO calculations[73,74] on hydrogen-bonded systems; these appear to be consistent with experimental data. Values of overlap populations in the same range as those obtained in this work have been invoked by Whangbo and Canadell[75] to account for intermolecular Te···Te contacts in organic metals and for the associated electronic properties. A further test of the ability of EH calculations to study weak interactions is given in the Appendix.

Spectral and Structural Modifications Produced by Enclathration. The variations in vibrational spectra upon enclathration are consistent with the hdyrogen-bonding model. The NH_3 stretching vibration is shifted to lower frequencies[33] by 21 cm^{-1} (3385 cm^{-1} in the host lattice, 3364 cm^{-1} in the clathrate), and a shift in the same direction by 66 cm^{-1} is observed for its bending mode (1230 cm^{-1} in the host, 1164 cm^{-1} in the clathrate). Notice that the N—H overlap population decreases 0.0017 upon enclathration, in good agreement with the decrease observed experimentally in the stretching frequency.

Table 4. Interatomic Distances (Å) in the $Ni_2(CN)_4(NH_3)_2$ Host Lattice,[20] in Benzene,[79] and in the $Ni_2(CN)_4(NH_3){\cdot}2C_6H_6$ Clathrate[62]

bond	sublattice	clathrate	difference
C—N	1.15(5)[a]	1.20(4)	+0.05
Ni—N(NH_3)	2.10(4)	2.06(6)	−0.04
Ni—N(CN)	2.11(4)	2.15(3)	+0.04
Ni—C(CN)	1.86(4)	1.76(4)	−0.10
C1—C2	1.399(1)	1.41	+0.01
C2—C2′	1.399(1)	1.38	−0.02

[a] Standard deviations in parentheses when available.

In further support of the model, some structural parameters are altered by clathrate formation (Table 4). The fact that the C—N distance increases upon enclathration, together with the shift of the corresponding stretching frequency[33,76,77] from 2170 to 2161 cm^{-1}, indicates a weakening of this bond. This experimental fact is in agreement with donation from the occupied π orbitals of benzene toward the bands located at 0–3 eV, which also have CN antibonding character. The C—N overlap population decreases by 0.0004 upon benzene enclathration, suggesting a slight weakening of this bond. Even if the variation in the experimental bond distance is comparatively large, it must be considered with caution given its large standard deviation.

The calculated changes in overlap populations are rather small. Since it is well-known that Slater orbitals represent poorly the long interatomic distance behavior of the wave function for second-row atoms, we have recalculated overlap populations by using a double-ξ basis set[78] for C and N atoms (see the Appendix). In most cases, the calculated overlap populations are quite similar to those calculated with a single-ξ basis. In particular, the calculated changes in OPs for the C—N bond are −0.0004 and −0.0003 with the single- and double-ξ basis sets, respectively.

The variations in experimental Ni—N(NH_3) and Ni—N(CN) bond distances are rather small and within experimental error.[20,62] Furthermore, the Ni—N(NH_3) and Ni—N(CN) stretching frequencies are practically unaltered by enclathration. Consistently, the calculated OPs for the same bonds are not altered by enclathration, as corresponds to the Ni—N nonbonding nature of the acceptor levels of the host lattice.

The Ni—C bond distance becomes 0.1 Å shorter after enclathration. Also, a slight increase of 4 cm^{-1} in the corresponding stretching frequency can be detected. In the theoretical analysis of the preceeding section, no sizeable charge transfer is observed involving Ni—C bonding or antibonding levels (only the empty σ system of benzene interacts rather weakly with Ni—C bonding bands). The calculated changes in this OP are +0.0003 (single-ξ) and +0.0017 (double-ξ). A careful analysis of the energy spectrum of the Ni—C overlap population indicates that the reinforcement of this bond is associated with charge transfer from π(CN) to σ^* levels of benzene (interaction 2 in **11a**).

Let us now look at changes in the structure of the benzene guest. The calculations indicate the following variations of overlap populations: 0.0002 for C2—C2′ (double-ζ, 0.0004) and −0.0004 for C1—C2 (double-ζ, −0.0007). Experimentally, changes in the bond distances of the enclathrated benzene molecule are within experimental error, but theory and experiment seem to go in the same direction: the benzene molecule is compressed along the *c* axis and elongated in the perpendicular direction (Table 4). This asymmetrization is due to the different participation of the

(70) Nishikiori, S.; Ratcliffe, C. I.; Ripmeester, J. A. *Can. J. Chem.* **1990**, *68*, 2270.
(71) Hamilton, W. C.; Ibers, J. A. *Hydrogen Bonding in Solids*; W. A. Benjamin: New York, 1968.
(72) Pimentel, G. C. McClellan, A. L. *The Hydrogen Bond*; W. H. Freeman and Co.: San Francisco, 1960.
(73) Adam, W.; Grimison, A.; Hoffmann, R.; Zuazaga de Ortiz, C. *J. Am. Chem. Soc.* **1968**, *90*, 1509.
(74) Morokuma, K.; Kato, H.; Yonezawa, T.; Fukui, K. *Bull. Chem. Soc. Jpn.* **1965**, *38*, 1263.
(75) Canadell, E.; Monconduit, L.; Evain, M.; Brec, R.; Rouxel, J.; Whangbo, M.-H. *Inorg. Chem.* **1993**, *32*, 10.
(76) Akyuz, S.; Dempster, A. B.; Morehouse, R. L.; Suzuki, S. *J. Mol. Struct.* **1973**, *17*, 105–125.
(77) Davies, J. E. D.; Dempster, A. B.; Morehouse, R. L. *Spectrochim. Acta* **1974**, *30A*, 1989–2004.
(78) Martin, J. D.; Canadell, E.; Batail, P. *Inorg. Chem.* **1992**, *31*, 3176.
(79) Cabana, A.; Bachand, J.; Giguère, J. *Can. J. Phys.* **1973**, *42*, 1949.

various benzene orbitals in the charge-transfer interactions. For example, the $1e_{1g}''$ orbital (Figure 11), C2–C2′ antibonding, donates more electron density than $1e_{1g}'$, C2—C2′ bonding. Also, the empty $1e_{2u}'$ orbital (C2—C2′ bonding) is the one receiving more electron density from the host lattice.

The out-of-plane bending vibrations of benzene are also sensitive to enclathration, their frequencies being larger in the clathrate than in free benzene.[80,81] This shift to higher frequencies has been assigned by some authors to weak hydrogen bonds between the hydrogen atoms of NH_3 and the π system of benzene.[77] Let us consider the out-of-plane normal vibration a_{2u}. It appears at 674 cm^{-1} for free benzene, at 705 cm^{-1} in the clathrate. From the EHTB total energies, we have calculated the corresponding force constant for free benzene, k_b, and in the clathrate, k_c, being $k_c/k_b = 1.11$ (see the Appendix for computational details). Since the wave number is related to the square root of the force constant, the calculated ratio for the wave numbers is $\nu_c/\nu_b = 1.05$, in excellent agreement with the ratio of the experimental frequencies, 1.04. It therefore appears that the EHTB calculations are able to detect weak host···guest interactions and correctly predict qualitatively the changes induced by enclathration in structural and vibrational parameters.

Discussion of the Results

In the previous section we have shown, through the analysis of the COD and ICOD functions, that the host···guest interactions in the Hofmann clathrate can be schematically described as occurring between the π electrons of the aromatic guest and the hydrogen atoms of the NH_3 groups in the host lattice and between the hydrogen atoms in the guest molecules and the cyanide groups in the host. At difference with classical hydrogen bonding, thought of as occurring between two electronegative atoms, such as N, O, F, or Cl, most of the host···guest interactions described here for the Hofmann clathrates involve a carbon atom and can be roughly grouped in two families: (a) those in which electron density is donated by a nonaromatic group (cyanide in the host lattice) and (b) those in which the electron donor is an aromatic molecule (benzene, pyrrole, or aniline).[11]

A survey of the literature, though, shows that "contacts" between hydrogen and carbon atoms are not that uncommon. Many such interactions have been experimentally characterized between acetylene or ethylene and water,[82,83] HF,[84,85] HCl,[86] or $O(CH_3)_2$[87] and between methane and HX (X = Cl, F, CN, SH).[88-90] Intermolecular complexes of benzene with water,[91,92] HF, or HCl[93,94] have also been described. It is important to point out that acetylene can interact with water either as an electron donor through its π system or as an electron acceptor through its hydrogen atoms, according to the results of SCF and SCF-MP2 calculations,[95,96] although only the latter geometry has been experimentally detected.[82] A compilation of neutron diffraction studies showing evidence of C—H···O, C—H···N, and C—H···Cl hydrogen bonds was reported by Taylor and Kennard.[97] Desiraju *et al.* have recently collected crystallographic evidence for CN···HC[98] and NH···phenyl contacts,[99] and Bernstein *et al.* have reviewed the importance of C—H···O and C—H···N hydrogen bonds for molecular conformation and packing.[100] The hydrogen bond is found to be sufficiently strong to stabilize the intermolecular complexes whose structure has been determined by diffraction methods. Even the electrical transport properties of complex crystal systems formed by clusters, BEDT-TTF molecules and guest solvent molecules, have been shown to be affected by hydrogen bonding.[101]

More closely related to the interactions present in the Hofmann clathrates are, for example, those found in stacks of TCNQ with intercalated benzene derivatives,[102] in which the CN groups act as donors toward the hydrogen atoms of benzene (dotted lines in **12**). In contrast, in compound **13**, the basic character corresponds

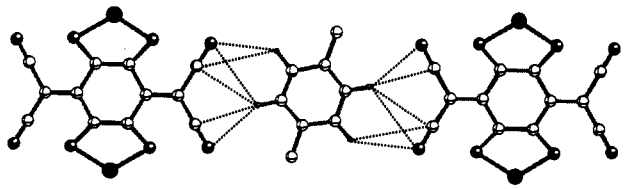

12

to the aromatic π system.[103] Recently, host···guest complexes

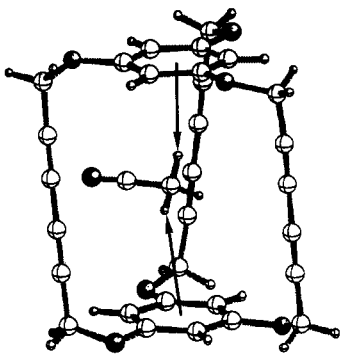

13

formed by the cyclic tetramer of resorcinol and alcohols have been reported.[104] In these complexes, the CH···$\pi(C_6H_6)$ interaction is estimated to contribute *ca.* 1.4 kcal/mol to the host···guest stabilization energy and accounts for the dependence of the NMR chemical shifts and the formation constants on the chain length of the alcohol. Further related systems can be found in the literature.[105-111]

(80) Wilson, E. B., Jr. *Phys. Rev.* **1934**, *5*, 706–714.
(81) Herzberg, G. *Infrared and Raman Spectra*; Van Nostrand-Reinhold: New York, 1945; Vol. 2.
(82) Peterson, K. I.; Klemperer, J. *J. Chem. Phys.* **1984**, *81*, 3842.
(83) Peterson, K. I.; Klemperer, J. *J. Chem. Phys.* **1986**, *85*, 725.
(84) Shea, J. A.; Flygare, W. H. *J. Chem. Phys.* **1982**, *76*, 4857.
(85) Biocchi, E. A.; Williams, J. H.; Klemperer, W. K. *J. Phys. Chem.* **1983**, *87*, 2681.
(86) Mootz, D.; Deeg, A. *J. Am. Chem. Soc.* **1992**, *114*, 5887.
(87) Jeng, M.-L. H.; Ault, B. *J. Phys. Chem.* **1990**, *94*, 4581.
(88) Legon, A. C.; Roberts, B. P.; Wallwork, A. L. *Chem. Phys. Lett.* **1990**, *173*, 107.
(89) Legon, A. C.; Wallwork, A. L. *J. Chem. Soc., Faraday Trans.* **1992**, *88*, 1.
(90) Woon, D. E.; Zeng, P.; Beck, D. R. *J. Chem. Phys.* **1990**, *98*, 11.
(91) Suzuki, S.; Green, P. G.; Bumgarner, R. E.; Dasgupta, S.; Goddard, W. A., III; Blake, G. A. *Science* **1992**, *257*, 942.
(92) Atwood, J. L.; Hamada, F.; Robinson, K. D.; Orr, W.; Vincent, R. L. *Nature* **1991**, *349*, 683.
(93) Read, W. G.; Campbell, E. J.; Henderson, G. J. *J. Chem. Phys.* **1983**, *78*, 3501.
(94) Klemperer, W. *Science* **1992**, *257*, 887.
(95) Frish, M. J.; Pople, J. A.; Del Bene, J. *J. Chem. Phys.* **1983**, *78*, 4063.
(96) Rovira, C.; Novoa, J. J. Submitted for publication.
(97) Taylor, R.; Kennard, O. *J. Am. Chem. Soc.* **1982**, *104*, 5063.
(98) Reddy, D. S.; Goud, B. S.; Panneerselvam, K.; Desiraju, G. R. *J. Chem. Soc., Chem. Commun.* **1993**, 663.
(99) Viswamitra, M. A.; Radhakrishnan, R.; Bandekar, J.; Desiraju, G. R. *J. Am. Chem. Soc.* **1993**, *115*, 4868.
(100) Bernstein, J.; Etter, M. C.; Leiserowitz, L. In *Structural Correlation*; Bürgi, H.-B., Dunitz, J. D., Eds.; VCH: Weinheim, 1994; Vol. 2, p 431–507.
(101) Pénicaud, A.; Boubekeur, K.; Batail, P.; Canadell, E.; Auban-Seuzier, P.; Jérome, D. *J. Am. Chem. Soc.* **1993**, *115*, 4101–4112.
(102) Suzuki, T.; Fujii, H.; Yamashita, Y.; Kabuto, C.; Tanaka, S.; Harasawa, M.; Mukai, T.; Miyashi, T. *J. Am. Chem. Soc.* **1992**, *114*, 3034.
(103) Berscheid, R.; Nieger, M.; Vögtle, F. *J. Chem. Soc., Chem. Commun.* **1991**, 1364.
(104) Kobayashi, K.; Asakawa, Y.; Kikuchi, Y.; Toi, H.; Aoyama, Y. *J. Am. Chem. Soc.* **1993**, *115*, 2648.
(105) Al-Karagouli, A. R.; Day, R. O.; Wood, J. S. *Inorg. Chem.* **1978**, *17*, 3702.
(106) Stephens, F. S.; Vagg, R. S. *Inorg. Chim. Acta* **1984**, *89*, 203.
(107) Corain, B.; Basato, M.; Favero, G.; Rosano, P. *Inorg. Chim. Acta* **1984**, *85*, L27.

Interactions between aromatic groups, analogous to those found between neighboring guest molecules in the Hofmann clathrates, have been extensively studied in the crystals of, for example, benzene[63] and naphthalene. In more complex systems, such as $[(AuC_6F_5)_2\{\mu\text{-}SPh_2PCHP(Ph_2Me)\}]$, depicted in **14**, aromatic

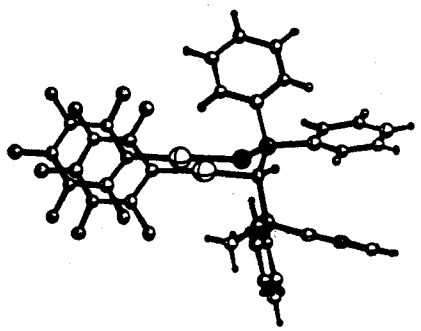

14

rings may be brought into proximity in different orientations: the pentafluorophenyl groups at the left are almost parallel, while the phenyl groups at the right try to avoid the parallel orientation.[112] A systematic study of interactions between aromatic rings, and of the substituent effects thereupon carried out recently by Sanders *et al.*,[64] has shown that the presence of the fluorine atoms bound to the phenyl ring decreases the ring···ring repulsions, thus allowing the parallel orientation. This suggests that the substituents in the aromatic guest molecules may vary their π density, thus influencing their enclathration properties.

With the simple interaction model **11** in mind, it is straightforward to conclude that the electron-donor or electron-withdrawing nature of the substituents of the benzene guest has a clear influence on the strength of the host···guest interaction. The most commonly used empirical parameter to calibrate substituent effects in aromatic compounds is the Hammett constant, σ_p^0. A large number of correlations between σ_p^0 and other properties have been established.[113] In particular, Siegel *et al.*[114] have found a linear correlation between the σ_p^0 parameter of the aryl groups in diarylnaphthalene and their rotational barriers, related to the inter-ring repulsions. It seems therefore interesting to look for a possible correlation between σ_p^0 of a guest molecule and its enclathration energy in a particular host lattice.

For the family of clathrates with a host lattice of $[Ni(NCS)_2(\alpha\text{-arylalkylamine})_4]$, similar to the Hofmann clathrates, a relationship has been found between σ_p^0 and the stability of the clathrates,[115] except for those cases in which the substituent is highly asymmetric, probably due to steric hindrance. A good correlation has recently been reported between the stability constants of α-cyclodextrin clathrates and the Hammett parameters of the substituents in the series of 1,4-disubstituted benzenes.[116] For the Hofmann clathrates with a host lattice of the type $Cd[NH_2(CH_2)_nNH_2]Ni(CN)_4$ (n = 2–7), Iwamoto *et al.*[117] have given a qualitative classification of the stabilities of systems with 51 different aromatic guest molecules. By analyzing such data according to the Hammett σ_p^0 parameters for the guest molecules, the following conclusions were drawn:

(a) Substituents of electron-rich character (those having a negative value of σ_p^0), such as NH_2 ($\sigma_p^0 = -0.38$), favor interaction of the aromatic system with the host, thus stabilizing the clathrate. Clathrates of aniline, toluidines, and xylidines have been prepared and yield stable crystals. CH_3 is another electron donor group ($\sigma_p^0 = -0.15$) which is found in the somewhat less stable clathrates of xylene.

(b) For monosubstituted rings with electron-deficient substituents (positive values of σ_p^0), such as the halogen atoms (F, σ_p^0 = 0.17; Cl, σ_p^0 = 0.27; Br, σ_p^0 = 0.29; I, σ_p^0 = 0.27), the corresponding clathrates have been prepared. Only in a few cases can unstable clathrates of disubstituted rings be obtained.

(c) Hofmann clathrates have not been obtained with guest aromatic molecules having strongly electron-deficient substituents, such as NO_2 (σ_p^0 = 0.83) or CN (σ_p^0 = 0.66).

The experimental data seems to be in agreement with the qualitative interaction model reported here. A more detailed analysis of the role of σ and π benzene components in the host···guest interaction has been carried out by means of ab initio calculations on bimolecular complexes, and a correlation between the calculated interaction energies for several clathrates and the Hammett parameters of the guest molecules has been found and will be reported elsewhere.[66]

Conclusions

Band calculations have been carried out on the Hofmann clathrate $Ni(NH_3)_2Ni(CN)_4{\cdot}2C_6H_6$, by using the extended Hückel tight-binding approximation. The crystal orbital displacement (COD) and integrated crystal orbital displacement (ICOD) functions defined here appear to be very useful for abstracting the relevant levels from a large set of noninteracting wave functions, therefore facilitating the detection of weak interactions between two sublattices in complex systems such as the Hofmann clathrates.

The orientation of the guest benzene molecule is predicted to present a rotation angle φ of 65°, in excellent agreement with the experimental angle of 65.9°. The orientation angle is seen to result from the interplay between the guest···guest and guest···axial ligand interactions. The calculated barrier for rotation of the guest molecule around the crystallographic c axis is 16 kJ/mol. Rotation of the benzene guest around its 6-fold axis is calculated to have a barrier of 16.2 kJ/mol, in excellent agreement with the experimental values in the range 15.0–16.2 kJ/mol.

The changes produced in the M—C and C—N bond distances of the host lattice and in the C—C distances of the guest molecule upon enclathration are nicely paralleled by the calculated changes in the corresponding overlap populations in EHTB calculations. An orbital explanation can be found for the fact that the benzene molecule is compressed along the c axis and stretched in the perpendicular direction. In contrast, the pyrrole guest molecule is elongated along the c axis in the corresponding clathrate.[11] Also changes in the vibrational spectra of both the host and the guest subsystems on enclathration are correctly predicted by the EHTB calculations: shifts to lower frequencies of the CN and N—H stretches, a shift to higher frequency of the Ni—C stretch, and, finally, the shift to higher wave numbers of the a_{2u} out-of-plane vibration of benzene.

In the benzene clathrate, the most important individual interaction corresponds to electron density transfer from the π orbital $1a_{2u}$ of benzene to empty orbitals of the host lattice, mostly the $3a_1$ and 2e (σ^* N–H) orbitals of the NH_3 groups. A resulting simplified description of the host···guest interactions would be that of a special type of "hydrogen bonds" between benzene and ammonia and between cyanide and benzene. In contrast, the

(108) Colapietro, M.; Domenicano, A.; Portalone, G.; Schultz, G.; Hargittai, I. *J. Mol. Struct.* **1984**, *112*, 141.
(109) Mosier-Boss, P. A.; Popov, A. I. *J. Am. Chem. Soc.* **1985**, *107*, 6168.
(110) Broderick, W. E.; Thompson, J. A.; Godfrey, M. R.; Sabat, M.; Hoffman, B. M. *J. Am. Chem. Soc.* **1989**, *111*, 7656.
(111) Hargittai, I.; Hargittai, M. *Mol. Struct. Energ.* **1987**, *2*, 1–35.
(112) Usón, R.; Laguna, A.; Laguna, M.; Fraile, M. N.; Lázaro, I.; Gimeno, M. C.; Jones, P. G.; Reihs, C.; Sheldrick, G. M. *J. Chem. Soc., Dalton Trans.* **1990**, 333.
(113) Duboc, C.; Ewing, D. F. In *Correlation Analysis in Chemistry*; Chapman, N. B., Shorter, J., Eds.; Plenum Press: New York, 1978.
(114) Cozzi, F.; Cinquini, M.; Annunziata, R.; Dwyer, T.; Siegel, J. S. *J. Am. Chem. Soc.* **1992**, *114*, 5729.
(115) Hanotier, J.; Radzitzky, P. d. In *Inclusion Compounds*; Atwood, J. L., Davies, J. E. D., MacNicol, D. D., Eds.; Academic Press: London, 1984; Vol. 1, p 19–57.
(116) Davies, D. M.; Savage, J. R. *J. Chem. Res. (S)* **1993**, 94.
(117) Nishikiori, S.; Ratcliffe, C. I.; Ripmeester, J. A. *J. Phys. Chem.* **1991**, *95*, 1589.

Table 5. Slater Exponents (ζ_μ) and Ionization Potentials ($H_{\mu\mu}$) for the Na Atomic Orbitals Used in the EHTB Calculations

atom	orbital	ζ_μ	$H_{\mu\mu}$ (eV)
Na	3s	1.40	-5.10
	3p	1.40	-3.00

metal atom does not participate significantly in the host···guest interaction. A similar explanation has been found for the pyrrole and aniline clathrates.[11] Consequently, the substituents in the guest molecule can vary the strength of the host···guest interactions by modifying the donor properties of its aromatic ring as measured by the Hammett σ_p^0 parameter, thereby enhancing the formation of hydrogen bonds with the lattice in the case of electron-rich substituents.

Acknowledgment. Financial support to this work was provided by DGICYT through Grant PB92–0655. The authors are grateful to the Centre de Supercomputació de Catalunya (CESCA) for the allocation of computer time, to F. Vilardell for expert help with the drawings, and to P. Alemany for suggestions and enlightening discussions.

Appendix: Computational Aspects

Extended Hückel calculations of molecular orbitals[118] and tight-binding bands[19,119] were carried out using the modified Wolfsberg–Helmholz formula.[120] Standard atomic parameters were used for C and H, N, and Ni.[118,121] The available Slater exponents for Na[122] yield orbitals which are too diffuse for an ionic situation in a solid-state calculation, therefore we have used a weighted average of the multi-ζ Mg^+ basis set of Clementi and Roetti[123] (Table 5). Slater exponents and coefficients for double-ζ atomic orbitals used in test calculations were also those of Clementi and Roetti.[123] COD and ICOD functions were calculated from DOS obtained by averaging throughout the irreducible wedge of the Brillouin zone, using meshes of 20 and 84 k-points for NaCl, 11 k-points for polyacetylene, and 120 k-points for the Hofmann clathrate.

The lattice parameter used in the calculations of the cubic NaCl crystal was a = 5.607 Å (space group $Fm3m$). The C—C distances in polyacetylene were taken as 1.40 Å for the regular chain and as 1.304 and 1.494 Å for the distorted one, with C—H distances of 1.09 Å. The experimental structure of the $Ni(NH_3)_2Ni(CN)_4{\cdot}2C_6H_6$ clathrate[62] was used for the host lattice. The complete unit cell of the $Ni(NH_3)_2Ni(CN)_4{\cdot}2C_6H_6$ clathrate was used for calculations of properties. For the calculation of COD functions, we used the simpler model $Ni(NH_3)_2Ni(CN)_4{\cdot}C_6H_6$, in which only half of the cavities are occupied by benzene molecules, to analyze the host···guest but not the guest···guest interactions. The structure adopted for the guest molecule of benzene was that of $Ni(NH_3)_2Ni(CN)_4{\cdot}2C_6H_6$.

Properties Calculation for the $t_{2g}^6e_g^n$ Electron Configurations. The Ni^{2+} ion in a slightly distorted octahedral environment is expected to have a $t_{2g}^6e_g^2$ electronic configuration. Hence, all the levels within its x^2-y^2 and z^2 bands should be half-occupied. Since the programs employed for band calculations always consider the electrons to be paired, we computed all properties as the average of those obtained for the configurations $t_{2g}^6e_g^0$ and $t_{2g}^6e_g^4$, as schematically shown in **15**.

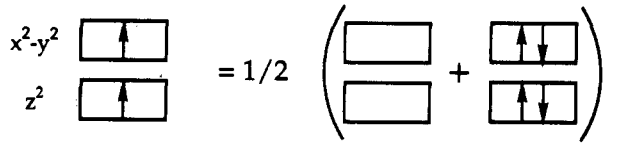

15

The effect of the electron configuration of the transition metal ions was checked by using a rigid band approximation for an $M(NH_3)_2Ni(CN)_4{\cdot}2C_6H_6$ clathrate. In such calculations, the occupation of the e_g bands was varied between 0 and 4, keeping the same atomic parameters used for M = Ni. Configurations with less d electrons could not be studied, since the computational method with the current parametrization does not allow the simultaneous consideration of occupied d bands of the square-planar metal atom and of t_{2g} bands of the octahedral metal lying in the same energy region (see Figure 8). The changes in electron configuration affected neither the optimized orientation of the benzene guest nor the relevant bonding parameters discussed above. Consequently, in the cases where occupied π orbitals of the guest appear in the same energy region as the half-occupied e_g orbitals of Ni(II), the electron configuration corresponding to Cd(II) was adopted for all property calculations to avoid artificial electron transfer from the guest π orbitals to e_g.

Since the large body of experience accumulated on extended Hückel calculations corresponds to chemically bonded systems, in which only large variations in the coefficients, overlap populations, or net charges are considered to be relevant, we wish to verify the significance of the small numerical values calculated for host···guest interactions in this paper within the extended Hückel formalism. In a paper devoted to the study of hydrogen bonding in the dimer of formic acid through EH calculations, Morokuma *et al.* reported[74] variations in the charge of the oxygen atom in the range 0.03–0.04, and of 0.03 in the O—H overlap population, at a relatively short intermolecular distance of 2.7 Å. These values are comparable to those found in the present work. On the other hand, the variation of the overlap populations and the potential energy as a function of the intermolecular angles, calculated at the EH level for the bimolecular $H_2O{\cdots}HCH_3$ system, correctly reproduces the qualitative behavior reported[124] by Novoa *et al.* at the SCF-MP2 level. Not unexpectedly, however, EH yields quantitative underestimates of such interactions, since the computed interaction energy at $O{\cdots}HCH_3$ = 2.3 Å is numerically equivalent to that obtained at the SCF-MP2 level at $O{\cdots}HCH_3$ = 2.8 Å. We believe that in the case of the Hofmann clathrates the exaggerated energy of the antibonding orbitals characteristic of EH calculations results in, for example, a very poor energy match of σ^*(N—H) with the occupied orbitals of benzene and a resulting small interaction energy.

The force constants for the a_{2u} out-of-plane mode of benzene, both in free benzene and in the $Ni(NH_3)_2Ni(CN)_4{\cdot}2C_6H_6$ clathrate, were calculated by performing small displacements of the hydrogen atoms around their equilibrium positions. The calculated energy was fitted to a parabola as a function of the displacement, and the second derivative was analytically derived. Given the relationship between force constant and wave number, $\nu \propto k^{1/2}$, the calculation of the ratio between the wave numbers for free and enclathrated benzene is straightforward.

(118) Hoffmann, R. *J. Chem. Phys.* **1963**, *39*, 1397.
(119) Whangbo, M.-H.; Hoffmann, R. *J. Am. Chem. Soc.* **1978**, *100*, 6093.
(120) Ammeter, J. H.; Bürgi, H.-B.; Thibeault, J. C.; Hoffmann, R. *J. Am. Chem. Soc.* **1978**, *100*, 3686.
(121) Summerville, R. H.; Hoffmann, R. *J. Am. Chem. Soc.* **1976**, *98*, 7240.
(122) Anderson, A. B.; Hoffmann, R. *J. Chem. Phys.* **1974**, *60*, 4271.
(123) Clementi, E.; Roetti, C. *At. Data Nucl. Data Tables* **1974**, *14*, 177.
(124) Novoa, J. J.; Tarrón, B.; Whangbo, M.-H.; Williams, J. M. *J. Chem. Phys.* **1991**, *95*, 5179.